Mathematics

https://www.aimspress.com/journal/Math

AIMS Mathematics, 11(7): 21541–21569.
DOI:10.3934/math.2026873
Received: 04 May 2026
Revised: 07 July 2026
Accepted: 10 July 2026
Published: 20 July 2026

Research article

Time-dependent optimal control of a SEITR spreading model with hesitation and truth mechanisms

Yuzhen Zhao[1], Jinling Wang[2,*] and Jiarong Li[3]

[1] College of Mathematics and Statistics, Northwest Normal University, Lanzhou 730070, China
[2] School of Science, Jimei University, Xiamen 361021, China
[3] College of Mathematics and System Sciences, Xinjiang University, Urumqi, 830046, China

* **Correspondence:** Email: jinling0803@126.com.

Abstract: This paper introduces a hesitation mechanism and true information spreaders to establish a Susceptible-Exposed-Infected-Truth-spreader-Recovered (SEITR) rumor propagation model, aiming to reveal how true information spreading influences rumor diffusion. First, based on the Routh-Hurwitz criterion and Lyapunov functions, the local asymptotic stability and global asymptotic stability of the system are proved respectively. Second, the Pontryagin minimum principle is applied to design the optimal control strategy, where key parameters are set as time-dependent functions, and the flexible control of the rumor propagation proportion is realized by dynamically adjusting control variables. Finally, numerical simulations verify the theoretical findings, which show that increasing the true information spreaders and blocking rumor transformation paths can effectively suppress rumor spread.

Keywords: rumor spreading; true information; basic reproduction number; stability analysis; optimal control
Mathematics Subject Classification: 34D05, 37N20

1. Introduction

A rumor is an unfounded statement fabricated and disseminated via various channels. With the rapid popularization of online social applications, the internet offers a virtual platform for global information exchange and brings great convenience to daily life. Nevertheless, it also fosters fast rumor diffusion, which may trigger risks to national security. Online rumors spread faster and reach wider audiences on social networks than traditional rumors. Thus, exploring rumor spreading mechanisms, analyzing its dynamic characteristics and designing effective containment strategies is of great significance.

The study of rumor propagation originated from epidemic dynamics. Given the similarities between the laws of rumor spread and the transmission mechanisms of infectious diseases, scholars have drawn on epidemic theories to investigate the propagation mechanism of rumors [1–3]. In 1965, Daley and Kendall proposed the DK model by taking into account the differences between rumor propagation and epidemic transmission [4]. By assuming that the transition probabilities between ignorants and spreaders conform to specific mathematical distributions, they analyzed rumor propagation via stochastic processes. In 1973, Maki and Thompson optimized the original transmission mechanism and put forward the MT model [5]. On this basis, numerous extended rumor propagation models have been derived in subsequent academic research [6–8].

With continuous research by scholars, rumor spread models have been continuously refined. Nekovee et al. expanded the rumor classification model based on group attributes [9]. Zanette first introduced complex network theory to construct a rumor spread model based on small-world networks, deriving conclusions such as the critical value for rumor spread [10, 11]. Jia et al. based on the SIR model, proposed a rumor spread model incorporating dual-channel (group and point-to-point) spread and improved the SIR model [12]. Wang et al. introduced the concept of "negative energy" to propose an improved energy model for controlling rumor spread [13]. Lan et al. extended the influencing factors of online rumors and identified key parameters for suppressing rumor spread [14]. Liu et al. developed a Susceptible-Exposed-Infected-Recovered (SEIR) rumor spread model for heterogeneous networks, finding that the rumor spread threshold is significantly influenced by network topology and analyzing its global dynamic behavior [15]. These studies aim to reveal the patterns of rumor spread and explore governance strategies, with extensive research conducted by numerous scholars [16–18].

Recent studies have further incorporated multiple realistic influencing factors such as rumor-refuting information and genuine information spreaders. Karumathil et al. constructed a rumor propagation model integrating media effect, forgetting and remembering mechanisms, and individual beliefs to uncover the interaction mechanisms of influencing factors [19]. Based on hypergraph theory, Li et al. proposed a Susceptible-Exposed-Informed-Antagonistic-Removed (SEIAR) rumor propagation model, which introduces antagonistic states on the basis of the classical SEIR model [20]. Du et al. established a Susceptible media-Debunking media-Removed media-Susceptible-Infected-Debunking-Removed (XYZ-SIDR) rumor propagation model with media rumor debunking, and analyzed its dynamic stability and time delay effects [21]. Zheng et al. constructed a rumor propagation model based on quantum superposition theory, analyzed the stability of equilibrium points, and quantified the impacts of public credulity degree and regulation intensity on the scale of rumor diffusion [22]. Wang et al. investigated the influence of genuine information spreaders on the transformation of public opinion groups, and proposed rumor-refuting regulation strategies combined with optimal control. Simulation results demonstrate that expanding the group of genuine information spreaders at an early stage can significantly curb rumor propagation [23]. Zhang et al. established a Susceptible-Infected-Truth-spreader-Recovered (SITR) rumor propagation model incorporating genuine information spreaders and forgetting factors. Numerical simulations verified the theoretical conclusions, revealing that the initial quantity of genuine information spreaders exerts a prominent effect on the peak value and duration of rumor prevalence [24].

Existing literature mostly constructs rumor suppression models from perspectives such as external media rumor refutation, spontaneous public resistance, and population memory decay. Although some studies incorporate compartments of truth spreaders or anti-rumor groups, they still have obvious limitations. First, the vast majority of models only introduce rumor-refuting individuals separately, ignoring the hesitant psychological state of netizens who wait and see, hesitate, and refrain from reposting after being exposed to rumors; these models lack coupled dynamics between hesitant compartments and genuine information spreaders. Second, the transformation paths from truth spreaders to various population groups are oversimplified, failing to characterize the complete interaction process in which susceptible, exposed, and rumor-spreading individuals convert into truth disseminators after contacting genuine information spreaders simultaneously. To address the above gaps in existing research, this paper introduces two compartments—hesitant individuals and genuine information spreaders, and establishes a Susceptible-Exposed-Infected-Truth-spreader-Recovered (SEITR) rumor propagation dynamic model.

Rumor spread is prone to out-of-control and social hazards, and optimal control theory can optimize rumor-refuting strategies to balance prevention efficiency and governance costs. In existing studies, Zhu et al. analyzed the diffusion of green behaviors by means of multilayer networks, Markov chains and reaction-diffusion models, and completed parameter identification via optimal control. Simulation experiments compare the identification performance of this method with convolutional neural networks [25]. Sha et al. established a reaction-diffusion model for rumor propagation, analyzed the evolution of network patterns based on Turing theory, and adopted optimal control for parameter identification. Simulations and real epidemic tweet data verify that the combination of government intervention and public discrimination capacity can effectively regulate rumors [26]. Mohamed et al. constructed a fractional-order optimal control model with three types of time-varying control strategies, and derived the necessary optimality conditions based on Pontryagin's maximum principle [27]. Jain et al. adopted the counter-information rumor suppression mechanism to establish an optimal control model, realizing the collaborative optimization of infected population scale and control cost [28]. Most objective functions in previous studies are linear or quadratic. To address these limitations, the optimal control strategy proposed in this paper introduces a discount factor, quadratic cost function, and three-dimensional time-varying control variables, which highlights the importance of early rumor intervention, remedies the defect of time effect homogenization, realizes differentiated cost regulation through weight parameters, and guarantees the uniqueness and stability of optimal solutions. Based on the above analysis, the innovations of this paper are summarized as follows:

(1) Compared with the existing literature [24,29], this paper introduces the compartment of genuine information spreaders and incorporates the individual hesitation mechanism to establish an SEITR rumor propagation system, which characterizes the interaction law of multi-path conversions from susceptible, hesitant, and rumor-spreading individuals to genuine information spreaders.

(2) This paper introduces a discount factor into the objective function of optimal control to characterize the difference in intervention value at different times, strengthen the control weight in the early stage of rumor diffusion, and combine three-dimensional time-varying control variables to effectively improve the timeliness of public opinion intervention.

(3) A quadratic cost function is constructed in the objective function of optimal control to realize the weighted optimal allocation of prevention and control costs, overcome the limitation of constant and equal cost weights in traditional control strategies, and ensure the uniqueness and stability of optimal control solutions.

The organization of this paper is as follows: Section 2 presents the establishment of an SEITR rumor propagation model. The stability of each equilibrium point is proved in Section 3. The optimal control strategy is proposed in Section 4. Theoretical verification is carried out via numerical simulations in Section 5. Finally, conclusions are drawn in Section 6.

2. Model formulation

The spread of rumors is affected by multiple factors. Individual hesitation directly influences the spread of rumors, while people who grasp the truth take the initiative to spread true information, which plays a positive role in curbing rumors. To this end, based on the classical SIR model, this paper introduces the exposed group and the true information spreader group and constructs an improved SEITR rumor propagation model.

Assume that $N(t)$ is the total population, which is divided into five categories: $S(t)$ represents the susceptible individuals who have never heard of the rumors; $E(t)$ represents the exposed individuals who have heard the rumors but have not yet spread them, but may become carriers of the rumors; $I(t)$ represents the spreaders who have heard and are spreading the rumors; $T(t)$ represents the true information spreaders; $R(t)$ represents the immune individuals who neither believe in nor spread the rumors. The spread mechanism of rumors in this model is as follows:

1) The number of newly added individuals per unit time is constant, referred to as the migration constant (Λ). All these newly added individuals are susceptible individuals, and the removal rate of all compartments is set to μ.

2) The contact rate between susceptible individuals and rumor spreaders is a constant ϕ. Upon contact, if an individual blindly believes and spreads the rumor without judgment, they transition to become spreaders with probability θ; if they adopt a skeptical attitude and do not spread the rumor, they become exposed individuals with probability (1-θ).

3) If exposed individuals accept and spread the rumors, they transition to become rumor spreaders with probability ρ. Over time, exposed individuals and rumor spreaders may transition to become immune individuals with probability ϵ due to losing interest in the rumors or forgetting them.

4) Susceptible individuals, exposed individuals, and rumor spreaders become truthful information spreaders with probability δ.

Based on the rumor spread mechanism, Λ, ϕ, θ, δ, ρ, ϵ, and μ are all positive constants. The meanings of these parameters are shown in Table 1, and we can draw a rumor spreading dynamics compartmental diagram as shown in Figure 1.

Table 1. Description of parameters in the model.

Parameter	Description
$\langle k \rangle$	Average degree of a homogeneous network
Λ	Number of susceptible individuals entering per unit of time
ϕ	The contact rate between susceptible individuals and rumor spreading individuals
θ	The conversion rate of susceptible individuals to rumor spreading individuals
δ	The conversion rates from susceptibles, the exposed, and spreaders to true information spreaders
ρ	The conversion rate from the exposed to rumor spreaders
ϵ	The conversion rates from the exposed and the rumor spreaders to the immunizers
μ	The emigration rates for different compartments

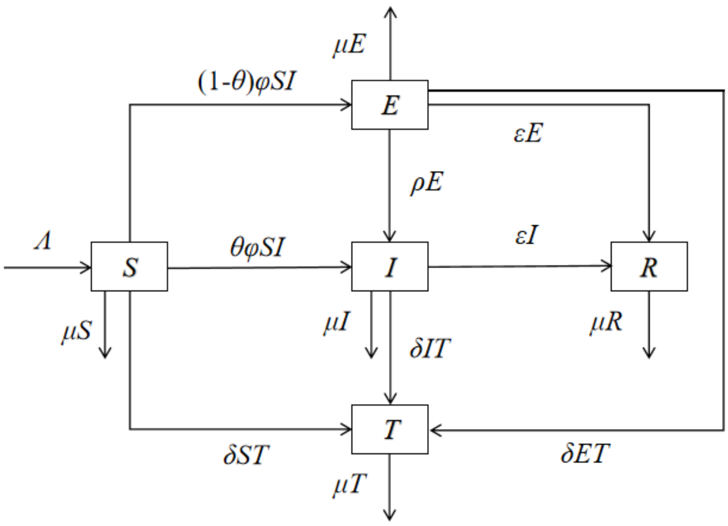

Figure 1. Rumor spreading dynamics compartmental diagram.

Therefore, the SEITR rumor spreading model can be expressed as follows:

$$\begin{cases} \dfrac{\mathrm{d}S(t)}{\mathrm{d}t} = \Lambda - \phi\langle k\rangle S(t)I(t) - \delta\langle k\rangle S(t)T(t) - \mu S(t), \\ \dfrac{\mathrm{d}E(t)}{\mathrm{d}t} = (1-\theta)\phi\langle k\rangle S(t)I(t) - \delta\langle k\rangle E(t)T(t) - \rho E(t) - \epsilon E(t) - \mu E(t), \\ \dfrac{\mathrm{d}I(t)}{\mathrm{d}t} = \theta\phi\langle k\rangle S(t)I(t) + \rho E(t) - \delta\langle k\rangle I(t)T(t) - \epsilon I(t) - \mu I(t), \\ \dfrac{\mathrm{d}T(t)}{\mathrm{d}t} = \delta\langle k\rangle T(t)(S(t)+E(t)+I(t)) - \mu T(t), \\ \dfrac{\mathrm{d}R(t)}{\mathrm{d}t} = \epsilon E(t) + \epsilon I(t) - \mu R(t), \end{cases} \tag{2.1}$$

with the initial conditions of the model

$$S(0) = S_0 \geq 0, \quad E(0) = E_0 \geq 0, \quad I(0) = I_0 \geq 0, \quad T(0) = T_0 \geq 0, \quad R(0) = R_0 \geq 0. \tag{2.2}$$

Since

$$N(t) = S(t) + E(t) + I(t) + T(t) + R(t),$$

we have

$$\lim_{t\to+\infty} \sup N(t) \leq \frac{\Lambda}{\mu}.$$

The positively invariant set of model (2.1) is given by

$$\Gamma = \left\{(S,E,I,T,R) \in \mathbb{R}^5,\ 0 \leq S(t) + E(t) + I(t) + T(t) + R(t) \leq \frac{\Lambda}{\mu}\right\}.$$

Obviously, we can find that the differential equations of $S(t)$, $E(t)$, $I(t)$, and $T(t)$ are independent of $R(t)$, For convenience, the model (2.1) can be reduced to the following equivalent form:

$$\begin{cases} \dfrac{\mathrm{d}S(t)}{\mathrm{d}t} = \Lambda - \phi\langle k\rangle S(t)I(t) - \delta\langle k\rangle S(t)T(t) - \mu S(t), \\ \dfrac{\mathrm{d}E(t)}{\mathrm{d}t} = (1-\theta)\phi\langle k\rangle S(t)I(t) - \delta\langle k\rangle E(t)T(t) - \rho E(t) - \epsilon E(t) - \mu E(t), \\ \dfrac{\mathrm{d}I(t)}{\mathrm{d}t} = \theta\phi\langle k\rangle S(t)I(t) + \rho E(t) - \delta\langle k\rangle I(t)T(t) - \epsilon I(t) - \mu I(t), \\ \dfrac{\mathrm{d}T(t)}{\mathrm{d}t} = \delta\langle k\rangle T(t)(S(t)+E(t)+I(t)) - \mu T(t), \end{cases} \tag{2.3}$$

3. Equilibrium points and stability analysis

In this section, we use the next-generation matrix method [30] to calculate the basic reproduction number R_0, determine the equilibrium points of model (2.3), and apply the Routh-Hurwitz criterion and the LaSalle invariance principle to analyze its stability.

3.1. The basic reproduction number R_0

To more accurately characterize the stability of the equilibrium point in the system, we introduce the basic reproduction number R_0.

First, let $X = (I(t), E(t), T(t), S(t))$, then model (2.3) can be written as

$$\frac{\mathrm{d}X}{\mathrm{d}t} = \mathcal{F}(X) - \mathcal{V}(X),$$

where

$$\mathcal{F}(X) = \begin{pmatrix} \theta\phi\langle k\rangle S(t)I(t) \\ (1-\theta)\phi\langle k\rangle S(t)I(t) \\ \delta\langle k\rangle T(t)(S(t)+E(t)+I(t)) \\ 0 \end{pmatrix},$$

$$\mathcal{V}(X) = \begin{pmatrix} -\rho E(t) + \delta\langle k\rangle I(t)T(t) + \epsilon I(t) + \mu I(t) \\ \delta\langle k\rangle E(t)T(t) + \rho E(t) + \epsilon E(t) + \mu E(t) \\ \mu T(t) \\ -\Lambda + \phi\langle k\rangle S(t)I(t) + \delta\langle k\rangle S(t)T(t) + \mu S(t) \end{pmatrix}.$$

Obviously, rumor-free equilibrium is $E_0 = (\frac{\Lambda}{\mu}, 0, 0, 0)$, and the Jacobian matrices of $\mathcal{F}(X)$ and $\mathcal{V}(X)$ are obtained at equilibrium E_0,

$$F(E_0) = \begin{pmatrix} \frac{\theta\phi\langle k\rangle\Lambda}{\mu} & 0 & 0 & 0 \\ \frac{(1-\theta)\phi\langle k\rangle\Lambda}{\mu} & 0 & 0 & 0 \\ 0 & 0 & \frac{\delta\langle k\rangle\Lambda}{\mu} & 0 \\ 0 & 0 & 0 & 0 \end{pmatrix}, \quad V(E_0) = \begin{pmatrix} \epsilon+\mu & -\rho & 0 & 0 \\ 0 & \rho+\epsilon+\mu & 0 & 0 \\ 0 & 0 & \mu & 0 \\ \frac{\phi\langle k\rangle\Lambda}{\mu} & 0 & \frac{\delta\langle k\rangle\Lambda}{\mu} & \mu \end{pmatrix}.$$

Further, it yields

$$FV^{-1} = \begin{pmatrix} \frac{\theta\phi\langle k\rangle\Lambda}{\mu(\epsilon+\mu)} & \frac{\theta\phi\langle k\rangle\Lambda\rho}{\mu(\epsilon+\mu)(\rho+\epsilon+\mu)} & 0 & 0 \\ \frac{(1-\theta)\phi\langle k\rangle\Lambda}{\mu(\epsilon+\mu)} & \frac{(1-\theta)\phi\langle k\rangle\Lambda\rho}{\mu(\epsilon+\mu)(\rho+\epsilon+\mu)} & 0 & 0 \\ 0 & 0 & \frac{\delta\langle k\rangle\Lambda}{\mu^2} & 0 \\ 0 & 0 & 0 & 0 \end{pmatrix}.$$

Finally, the basic reproduction number of model (2.3) is

$$R_0 = \max\{\rho(FV^{-1})\} = \max\{R_{01}, R_{02}\},$$

where $R_{01} = \frac{\phi\langle k\rangle\Lambda(\theta\epsilon+\theta\mu+\rho)}{\mu(\epsilon+\mu)(\rho+\epsilon+\mu)}$, $R_{02} = \frac{\delta\langle k\rangle\Lambda}{\mu^2}$.

Remark 1. *The stability of a system's equilibrium is often assessed through a critical threshold known as the basic reproduction number R_0. It represents the average number of new individuals that a single infected person can infect during the infectious period. If $R_0 > 1$, the system is in an unstable state, and the spread of rumors will continue. Conversely, if $R_0 < 1$, the spread of rumors will gradually weaken, and the system will tend toward stability, or even the complete disappearance of the rumors.*

3.2. Stability analysis of the rumor-free equilibrium E_0

Theorem 3.1. *The rumor-free equilibrium E_0 is locally asymptotically stable if $R_0 < 1$.*

Proof. The Jacobian matrix at E_0 is

$$J(E_0) = \begin{pmatrix} -\mu & 0 & -\frac{\theta\langle k\rangle\Lambda}{\mu} & -\frac{\delta\langle k\rangle\Lambda}{\mu} \\ 0 & -(\rho+\epsilon+\mu) & \frac{(1-\theta)\phi\langle k\rangle\Lambda}{\mu} & 0 \\ 0 & \rho & \frac{\theta\phi\langle k\rangle\Lambda}{\mu} - (\epsilon+\mu) & 0 \\ 0 & 0 & 0 & \mu(R_{02}-1) \end{pmatrix}.$$

The characteristic equation of matrix $J(E_0)$ is

$$|h - J(E_0)| = (h+\mu)(h-\mu(R_{02}-1))(h^2 + a_1 h + a_0) = 0, \tag{3.1}$$

where $a_1 = (\epsilon+\mu)(1 - \frac{\theta\phi\langle k\rangle\Lambda}{\mu(\epsilon+\mu)}) + \rho + \epsilon + \mu, a_0 = (\epsilon+\mu)(\rho+\epsilon+\mu)(1-R_{01})$.

Therefore, two characteristic roots corresponding to the characteristic equation of $J(E_0)$ is $h_{01} = -\mu < 0, h_{02} = \mu(R_{02}-1) < 0$, and the remaining characteristic roots fulfill the equation as stated below:

$$h^2 + a_1 h + a_0 = 0. \tag{3.2}$$

If $R_{01} < 1$, then $\frac{\theta\phi\langle k\rangle\Lambda}{\mu(\epsilon+\mu)} < 1$, thus $a_1 > 0$ and $a_0 > 0$. That is, both roots of Eq (3.2) are negative real roots. According to the Routh-Hurwitz criterion [31], E_0 is locally asymptotically stable if $R_0 < 1$. □

Theorem 3.2. *The rumor-free equilibrium E_0 of the model (2.3) is globally asymptotically stable if $\frac{\phi\langle k\rangle\Lambda}{\mu(\epsilon+\mu)} < 1$ and $R_{02} < 1$.*

Proof. Define the Lyapunov function

$$V(t) = S - S^* - S^* \ln\frac{S}{S^*} + E + I + T,$$

where $S^* = \frac{\Lambda}{\mu}$. Thus, the derivative of V(t) along the positive solutions of model (2.3) is

$$\begin{aligned}\frac{dV(t)}{dt} \;&=\; (1 - \frac{S^*}{S})\left[-\phi\langle k\rangle SI - \delta\langle k\rangle ST + \mu(S^* - S)\right] + (1-\theta)\phi\langle k\rangle SI \\ &\quad -\delta\langle k\rangle ET - \rho E - \epsilon E - \mu E + \theta\phi\langle k\rangle SI + \rho E - \delta\langle k\rangle IT - \epsilon I\end{aligned}$$

$$
\begin{aligned}
& -\mu I+\delta\langle k\rangle T(S+E+I)-\mu T \\
= \ & \phi\langle k\rangle S^* I+\delta\langle k\rangle S^* T-\frac{\mu}{S}(S^*-S)^2-(\epsilon+\mu)E-(\epsilon+\mu)I-\mu T \\
\leq \ & -(\epsilon+\mu)E+\left[\frac{\phi\langle k\rangle\Lambda}{\mu(\epsilon+\mu)}-1\right]I+(R_{02}-1)T.
\end{aligned}
$$

When $\frac{\phi\langle k\rangle\Lambda}{\mu(\epsilon+\mu)}<1$ and $R_{02}<1$, then $\frac{\mathrm{d}V(t)}{\mathrm{d}t}\leq 0$ for all $E(t), I(t), T(t)\geq 0$, if and only if $E(t)=0, I(t)=0$, $T(t)=0$, $\frac{\mathrm{d}V(t)}{\mathrm{d}t}=0$. According to the LaSelle's invariance principle [32], we draw the conclusion that E_0 is globally asymptotically stable when $\frac{\phi\langle k\rangle\Lambda}{\mu(\epsilon+\mu)}<1$ and $R_{02}<1$. □

Remark 2. *In Theorem 3.1, the equilibrium point E_0 is locally asymptotically stable when $R_0<1$, In Theorem 3.2, the global asymptotic stability condition for E_0 is given by $\frac{\phi\langle k\rangle\Lambda}{\mu(\epsilon+\mu)}<1$ and $R_{02}<1$. Since $\frac{\phi\langle k\rangle\Lambda}{\mu(\epsilon+\mu)}<1$ is a sufficient but not necessary condition for $R_{01}<1$, this implies that the global asymptotic stability condition in Theorem 3.2 is more relaxed than the local asymptotic stability condition in Theorem 3.1.*

3.3. Stability analysis of boundary equilibrium E_1

During rumor spreading, the crowd is eventually devoid of rumor spreaders due to the presence of true information spreaders. When $I=0$ and $T\neq 0$, the boundary equilibrium satisfies

$$
\begin{cases}
\Lambda-\delta\langle k\rangle ST-\mu S=0, \\
-\delta\langle k\rangle ET-\rho E-\epsilon E-\mu E=0, \\
\rho E=0, \\
\delta\langle k\rangle T(S+E)-\mu T=0.
\end{cases} \tag{3.3}
$$

According to the calculation, if $R_{01}<1$ and $R_{02}>1$, the boundary equilibrium point $E_1=(\frac{\mu}{\delta\langle k\rangle}, 0, 0, \frac{\mu(R_{02}-1)}{\delta\langle k\rangle})$ exists.

Theorem 3.3. *The boundary equilibrium E_1 is locally asymptotically stable if $R_{01}<1$, $R_{02}>1$, and $\phi<\frac{\delta\left[\mu R_{02}(\mu R_{02}+\rho+2\epsilon)+\epsilon^2+\rho\epsilon\right]}{\mu(\theta\mu R_{02}+\rho+\theta\epsilon)}$.*

Proof. The Jacobian matrix at E_1 is

$$
J(E_1)=\begin{pmatrix}
-\mu R_{02} & 0 & -\frac{\phi\mu}{\delta} & -\mu \\
0 & -\mu R_{02}-\rho-\epsilon & \frac{(1-\theta)\phi\mu}{\delta} & 0 \\
0 & \rho & \frac{\theta\phi\mu}{\delta}-\mu R_{02}-\epsilon & 0 \\
\mu R_{02}-\mu & \mu R_{02}-\mu & \mu R_{02}-\mu & 0
\end{pmatrix}.
$$

The characteristic equation of matrix $J(E_1)$ is

$$
|h-J(E_1)|=(h^2+\mu R_{02}h+\mu^2(R_{02}-1))(h^2+b_1h+b_0)=0, \tag{3.4}
$$

where

$$
b_1=2\mu R_{02}-\frac{\theta\phi\mu}{\delta}+2\epsilon+\rho,
$$

$$
b_0=\mu R_{02}(\mu R_{02}+\rho+2\epsilon)+\epsilon^2+\rho\epsilon-\frac{\theta\phi\mu^2R_{02}+\phi\mu\rho+\theta\phi\mu\epsilon}{\delta}.
$$

Obviously, there are four characteristic roots, and the equations satisfied by two characteristic roots are as follows:

$$(h^2 + \mu R_{02} h + \mu^2 (R_{02} - 1)) = 0, \tag{3.5}$$

the other two characteristic roots are satisfied by the following equations:

$$(h^2 + b_1 h + b_0) = 0. \tag{3.6}$$

For Eq (3.5), if $R_{02} > 1$, then both roots are negative real roots.

For Eq (3.6), if $\phi < \frac{\delta[\mu R_{02}(\mu R_{02}+\rho+2\epsilon)+\epsilon^2+\rho\epsilon]}{\mu(\theta\mu R_{02}+\rho+\theta\epsilon)}$, then $b_0 > 0$ and $b_1 > 0$. Equation (3.6) has two negative real characteristic roots.

Therefore, in light of the Routh-Hurwitz stability criterion [31], the boundary equilibrium E_1 is locally asymptotically stable, if $R_{01} < 1$, $R_{02} > 1$, and $\phi < \frac{\delta[\mu R_{02}(\mu R_{02}+\rho+2\epsilon)+\epsilon^2+\rho\epsilon]}{\mu(\theta\mu R_{02}+\rho+\theta\epsilon)}$. □

Theorem 3.4. *The boundary equilibrium E_1 of the model* (2.3) *is globally asymptotically stable if $R_{01} < 1$ and $R_{02} > \max\{1, \frac{\phi\mu-\delta\epsilon}{\delta\mu}\}$.*

Proof. Construct the Lyapunov function

$$V(t) = V_1(t) + V_2(t) + V_3(t) + V_4(t),$$

where

$$V_1(t) = S - S^* - S^* \ln \frac{S}{S^*}, V_2(t) = E, V_3(t) = I, V_4(t) = T - T^* - T^* \ln \frac{T}{T^*}.$$

The derivative of the above equations along the positive solutions of model (2.3) are

$$\begin{aligned}
\frac{\mathrm{d}V_1(t)}{\mathrm{d}t} &= (1 - \frac{S^*}{S})(\Lambda - \phi \langle k\rangle SI - \delta \langle k\rangle ST - \mu S) \\
&= (1 - \frac{S^*}{S})(\delta \langle k\rangle S^*T^* + \mu S^* - \phi \langle k\rangle SI - \delta \langle k\rangle ST - \mu S) \\
&= (1 - \frac{S^*}{S})[\delta \langle k\rangle S^*T^*(1 - \frac{ST}{S^*T^*}) - \phi \langle k\rangle SI + \mu(S^* - S)] \\
&= \delta \langle k\rangle S^*T^*(1 - \frac{ST}{S^*T^*} - \frac{S^*}{S} + \frac{T}{T^*}) - \phi \langle k\rangle SI + \phi \langle k\rangle S^*I - \frac{\mu}{S}(S^* - S)^2, \\
\frac{\mathrm{d}V_2(t)}{\mathrm{d}t} &= (1 - \theta)\phi \langle k\rangle SI - \delta \langle k\rangle ET - \rho E - \epsilon E - \mu E, \\
\frac{\mathrm{d}V_3(t)}{\mathrm{d}t} &= \theta\phi \langle k\rangle SI + \rho E - \delta \langle k\rangle IT - \epsilon I - \mu I, \\
\frac{\mathrm{d}V_4(t)}{\mathrm{d}t} &= (1 - \frac{T^*}{T})[\delta \langle k\rangle T(S + E + I) - \mu T] \\
&= (1 - \frac{T^*}{T})[\delta \langle k\rangle T(S + E + I) - \delta \langle k\rangle S^*T] \\
&= (1 - \frac{T^*}{T})[\delta \langle k\rangle S^*T^*(\frac{ST}{S^*T^*} - \frac{T}{T^*}) + \delta \langle k\rangle T(E + I)] \\
&= \delta \langle k\rangle S^*T^*(\frac{ST}{S^*T^*} - \frac{T}{T^*} - \frac{S}{S^*} + 1) + (1 - \frac{T^*}{T})\delta \langle k\rangle T(E + I).
\end{aligned}$$

Further calculations show that

$$\begin{aligned}
\frac{dV(t)}{dt} &= -\frac{\delta\langle k\rangle T^*}{S}(S^*-S)^2+\phi\langle k\rangle S^*I-\frac{\mu}{S}(S^*-S)^2-\epsilon E-\mu E-\epsilon I-\mu I-\delta\langle k\rangle T^*(E+I)\\
&\leq \phi\langle k\rangle S^*I-(\epsilon+\mu)E-(\epsilon+\mu)I-\delta\langle k\rangle T^*(E+I)\\
&= -(\mu R_{02}+\epsilon)E+(\frac{\phi\mu}{\delta}-\epsilon-\mu R_{02})I.
\end{aligned}$$

When $R_{02}>\max\{1,\frac{\phi\mu-\delta\epsilon}{\delta\mu}\}$, then $\frac{\phi\mu}{\delta}-\epsilon-\mu R_{02}<0$, thus $\frac{dV}{dt}\leq 0$ for all $E(t), I(t)\geq 0$, if and only if $E(t)$=0, $I(t)=0$, $\frac{dV}{dt}=0$. According to LaSelle's invariance principle [32], we draw the conclusion that the boundary equilibrium E_1 is globally asymptotically stable when $R_{01}<1$ and $R_{02}>\max\{1,\frac{\phi\mu-\delta\epsilon}{\delta\mu}\}$. □

3.4. Stability analysis of boundary equilibrium E_2

When $I\neq 0$, $T=0$, the boundary equilibrium satisfies

$$\begin{cases}\Lambda-\phi\langle k\rangle SI-\mu S=0,\\ (1-\theta)\phi\langle k\rangle SI-\rho E-\epsilon E-\mu E=0,\\ \theta\phi\langle k\rangle SI+\rho E-\epsilon I-\mu I=0.\end{cases}\tag{3.7}$$

Through calculation, the boundary equilibrium $E_2=(\frac{\Lambda}{\mu R_{01}},\frac{\Lambda(1-\theta)(R_{01}-1)}{(\rho+\epsilon+\mu)R_{01}},\frac{\mu(R_{01}-1)}{\phi\langle k\rangle},0)$ exists when R_{01}>1 and $R_{02}<1$.

Theorem 3.5. *The boundary equilibrium E_2 of the model* (2.3) *is locally asymptotically stable if R_{01}>1 and $R_{02}<\min\{1,\frac{\phi\langle k\rangle\Lambda R_{01}(\rho+\epsilon+\mu)}{(\rho+\epsilon+\mu)[\phi\langle k\rangle\Lambda+\mu^2R_{01}(R_{01}-1)]+\phi\langle k\rangle\Lambda\mu(1-\theta)(R_{01}-1)}\}$.*

Proof. The Jacobian matrix at E_2 is

$$J(E_2)=\begin{pmatrix}-\mu R_{01} & 0 & -\frac{\phi\langle k\rangle\Lambda}{\mu R_{01}} & -\frac{\delta\langle k\rangle\Lambda}{\mu R01}\\ (1-\theta)\mu(R_{01}-1) & -\rho-\epsilon-\mu & \frac{(1-\theta)\phi\langle k\rangle\Lambda}{\mu R_{01}} & \frac{-\delta\langle k\rangle\Lambda(1-\theta)(R_{01}-1)}{R_{01}(\rho+\epsilon+\mu)}\\ \theta\mu(R_{01}-1) & \rho & \frac{\theta\phi\langle k\rangle\Lambda}{\mu R_{01}}-\epsilon-\mu & -\frac{\delta\mu(R_{01}-1)}{\phi}\\ 0 & 0 & 0 & \delta\langle k\rangle\zeta-\mu\end{pmatrix}.$$

The characteristic equation of matrix $J(E_2)$ is

$$|h-J(E_2)|=(h-\delta\langle k\rangle\zeta+\mu)(h^3+c_2h^2+c_1h+c_0)=0.\tag{3.8}$$

It is easy to obtain $h_{21}=\delta\langle k\rangle\zeta-\mu$, where $\zeta=(\frac{\Lambda}{\mu R_{01}}+\frac{\Lambda(1-\theta)(R_{01}-1)}{(\rho+\epsilon+\mu)R_{01}}+\frac{\mu(R_{01}-1)}{\phi\langle k\rangle})$. Furthermore, if $R_{02}<\frac{\phi\langle k\rangle\Lambda R_{01}(\rho+\epsilon+\mu)}{(\rho+\epsilon+\mu)[\phi\langle k\rangle\Lambda+\mu^2R_{01}(R_{01}-1)]+\phi\langle k\rangle\Lambda\mu(1-\theta)(R_{01}-1)}$, then $h_{21}<0$.

The remaining characteristic roots satisfy the following equation:

$$h^3+c_2h^2+c_1h+c_0=0,\tag{3.9}$$

where $c_2=\mu R_{01}+(\epsilon+\mu)(1-\frac{D}{R_{01}})+(\rho+\epsilon+\mu)$, $c_1=\mu R_{01}(\rho+\epsilon+\mu)+\mu(\epsilon+\mu)(R_{01}-\frac{D}{R_{01}})$, $c_0=\mu(\epsilon+\mu)(\rho+\epsilon+\mu)(R_{01}-1)$, and $D=\frac{\theta\phi\langle k\rangle\Lambda}{\mu(\epsilon+\mu)}$.

Then, one has

$$
\begin{aligned}
\Delta_1 &= c_2 = \mu R_{01} + (\epsilon+\mu)\left(1-\frac{D}{R_{01}}\right) + (\rho+\epsilon+\mu),\\
\Delta_2 &= \begin{vmatrix} c_2 & 1 \\ c_0 & c_1 \end{vmatrix} = c_2c_1 - c_0\\
&= \mu(\epsilon+\mu)^2\left(1-\frac{D}{R_{01}}\right)\left(R_{01}-\frac{D}{R_{01}}\right) + \mu^2(\rho+\epsilon+\mu)R_{01}^2\\
&\quad + \mu^2(\epsilon+\mu)(R_{01}^2-D) + \mu(\epsilon+\mu)(\rho+\epsilon+\mu)\left(1-\frac{D}{R_{01}}\right)\\
&\quad + \mu(\epsilon+\mu)(\rho+\epsilon+\mu)(R_{01}-D) + \mu(\rho+\epsilon+\mu)^2R_{01}.
\end{aligned}
$$

If $R_{01} > 1$ and $D < R_{01}$, then $c_0 > 0$, $c_1 > 0$, $c_2 > 0$, $\Delta_1 > 0$, and $\Delta_2 > 0$. Thus, there are no positive roots for Eq (3.9). According to the Routh-Hurwitz stability criterion [31], when $R_{01} > 1$ and $R_{02} < \min\{1, \frac{\phi\langle k\rangle\Lambda R_{01}(\rho+\epsilon+\mu)}{(\rho+\epsilon+\mu)[\phi\langle k\rangle\Lambda+\mu^2R_{01}(R_{01}-1)]+\phi\langle k\rangle\Lambda\mu(1-\theta)(R_{01}-1)}\}$, the boundary equilibrium E_2 is locally asymptotically stable. □

3.5. Stability analysis of the endemic equilibrium E_3

When $I \neq 0$ and $T \neq 0$, the endemic equilibrium satisfies

$$
\begin{cases}
\Lambda - \phi\langle k\rangle SI - \delta\langle k\rangle ST - \mu S = 0,\\
(1-\theta)\phi\langle k\rangle SI - \delta\langle k\rangle ET - \rho E - \epsilon E - \mu E = 0,\\
\theta\phi\langle k\rangle SI + \rho E - \delta\langle k\rangle IT - \epsilon I - \mu I = 0,\\
\delta\langle k\rangle T(S+E+I) - \mu T = 0.
\end{cases} \tag{3.10}
$$

According to the above formula, E^*, I^*, and T^* can be expressed in terms of S^* as follows:

$$
E^* = \frac{(1-\theta)\phi\rho\mu^2\langle k\rangle S^*(\mu-\delta\langle k\rangle S^*)}{\delta\langle k\rangle((\delta\epsilon\langle k\rangle-\theta\phi\mu\langle k\rangle)S^*+\rho\mu+\Lambda\delta\langle k\rangle)(\Lambda\delta\langle k\rangle+\delta\epsilon\langle k\rangle S^*+\rho\mu)},
$$

$$
I^* = \frac{(\mu-\delta\langle k\rangle S^*)\rho\mu}{\delta\langle k\rangle((\delta\epsilon\langle k\rangle-\theta\phi\mu\langle k\rangle)S^*+\rho\mu+\Lambda\delta\langle k\rangle)},
$$

$$
T^* = \frac{\Lambda\delta\langle k\rangle-(\epsilon+\mu)\mu+\delta\epsilon\langle k\rangle S^*}{\delta\mu\langle k\rangle},
$$

and S^* satisfies

$$
d_2S^{*2} + d_1S^* + d_0 = 0, \tag{3.11}
$$

where $d_0 = -\Lambda^2\delta^2\langle k\rangle - \Lambda\delta\rho\mu$, $d_1 = \Lambda\theta\phi\delta\mu\langle k\rangle - 2\Lambda\delta^2\epsilon\langle k\rangle + \phi\rho\mu^2 - \delta\rho\epsilon\mu$, and $d_2 = \theta\phi\delta\epsilon\mu\langle k\rangle - \delta^2\epsilon^2\langle k\rangle$.

The existence of a positive root for Eq (3.11) depends on the following two scenarios:

Case 1. When $\frac{\theta\phi\mu}{\delta\epsilon} > 1$, then $d_2 > 0$. Because $d_0 < 0$, then the discriminant of Eq (3.11) is $\Delta > 0$, thus, Eq (3.11) has only one positive root E_3.

Case 2. When $\frac{\theta\phi\mu}{\delta\epsilon} < 1$, then $d_2 < 0$. When $\frac{\Lambda\theta\phi\delta\mu\langle k\rangle+\phi\rho\mu^2}{2\Lambda\delta^2\epsilon\langle k\rangle+\delta\rho\epsilon\mu} > 1$, then $d_1 > 0$. And when $\Delta > 0$, Eq (3.11) has two unique positive roots E_4 and E_5.

Theorem 3.6. *The endemic equilibrium E_3 of the model* (2.3) *is globally asymptotically stable if* $\frac{\theta\phi\mu}{\delta\epsilon}>1$ *and* $R_0 > 1$.

Proof. Construct a Lyapunov function

$$V = \frac{1}{(1-\theta)\phi\langle k\rangle S^*I^* + \rho E^*}(V_1 + V_2 + V_3 + V_4),$$

where

$$V_1(t) = S - S^* - S^* \ln\frac{S}{S^*}, V_2(t) = E - E^* - E^* \ln\frac{E}{E^*},$$
$$V_3(t) = I - I^* - I^* \ln\frac{I}{I^*}, V_4(t) = T - T^* - T^* \ln\frac{T}{T^*}.$$

Calculate the derivatives of the above equations along the trajectory of model (2.3):

$$\begin{aligned}
\frac{\mathrm{d}V_1(t)}{\mathrm{d}t} &= (1-\frac{S^*}{S})(\Lambda - \phi\langle k\rangle SI - \delta\langle k\rangle ST - \mu S)\\
&= (1-\frac{S^*}{S})(\phi\langle k\rangle S^*I^* + \delta\langle k\rangle S^*T^* + \mu S^* - \phi\langle k\rangle SI - \delta\langle k\rangle ST - \mu S)\\
&= (1-\frac{S^*}{S})[\phi\langle k\rangle S^*I^*(1-\frac{SI}{S^*I^*}) + \delta\langle k\rangle S^*T^*(1-\frac{ST}{S^*T^*}) + \mu(S^* - S)]\\
&= \phi\langle k\rangle S^*I^*(1-\frac{SI}{S^*I^*} - \frac{S^*}{S} + \frac{I}{I^*}) + \delta\langle k\rangle S^*T^*(1-\frac{ST}{S^*T^*} - \frac{S^*}{S} + \frac{T}{T^*}) + \mu S^*(2-\frac{S}{S^*} - \frac{S^*}{S}),\\
\frac{\mathrm{d}V_2(t)}{\mathrm{d}t} &= (1-\frac{E^*}{E})[(1-\theta)\phi\langle k\rangle SI - \delta\langle k\rangle ET - \rho E - \epsilon E - \mu E]\\
&= (1-\frac{E^*}{E})[(1-\theta)\phi\langle k\rangle SI - \delta\langle k\rangle ET - \frac{(1-\theta)\phi\langle k\rangle S^*I^* - \delta\langle k\rangle E^*T^*}{E^*}E]\\
&= (1-\frac{E^*}{E})[(1-\theta)\phi\langle k\rangle (SI - S^*I^*\frac{E}{E^*}) + \delta\langle k\rangle (E^*T^*\frac{E}{E^*} - ET)]\\
&= (1-\frac{E^*}{E})[(1-\theta)\phi\langle k\rangle S^*I^*(\frac{SI}{S^*I^*} - \frac{E}{E^*}) + \delta\langle k\rangle E^*T^*(\frac{E}{E^*} - \frac{ET}{E^*T^*})]\\
&= (1-\theta)\phi\langle k\rangle S^*I^*(\frac{SI}{S^*I^*} - \frac{E}{E^*} - \frac{SIE^*}{S^*I^*E} + 1) + \delta\langle k\rangle E^*T^*(\frac{E}{E^*} - \frac{ET}{E^*T^*} - 1 + \frac{T}{T^*}),\\
\frac{\mathrm{d}V_3(t)}{\mathrm{d}t} &= (1-\frac{I^*}{I})(\theta\phi\langle k\rangle SI + \rho E - \delta\langle k\rangle IT - \epsilon I - \mu I)\\
&= (1-\frac{I^*}{I})(\theta\phi\langle k\rangle SI + \rho E - \delta\langle k\rangle IT - \frac{\theta\phi\langle k\rangle S^*I^* + \rho E^* - \delta\langle k\rangle I^*T^*}{I^*}I)\\
&= (1-\frac{I^*}{I})[\theta\phi S^*I^*(\frac{SI}{S^*I^*} - \frac{I}{I^*}) + \rho E^*(\frac{E}{E^*} - \frac{I}{I^*}) - \delta\langle k\rangle I^*T^*(\frac{IT}{I^*T^*} - \frac{I}{I^*})]\\
&= \theta\phi\langle k\rangle S^*I^*(\frac{SI}{S^*I^*} - \frac{I}{I^*} - \frac{S}{S^*} + 1) + \rho E^*(\frac{E}{E^*} - \frac{I}{I^*} - \frac{I^*E}{IE^*} + 1)\\
&\quad -\delta\langle k\rangle I^*T^*(\frac{IT}{I^*T^*} - \frac{I}{I^*} - \frac{T}{T^*} + 1),\\
\frac{\mathrm{d}V_4(t)}{\mathrm{d}t} &= (1-\frac{T^*}{T})[\delta\langle k\rangle T(S + E + I) - \mu T]\\
&= (1-\frac{T^*}{T})[\delta\langle k\rangle T(S + E + I) - \delta\langle k\rangle (S^* + E^* + I^*)T]
\end{aligned}$$

$$
\begin{aligned}
&= (1-\frac{T^*}{T})[\delta\langle k\rangle(TS - T^*S^*\frac{T}{T^*}) + \delta\langle k\rangle(TE - T^*E^*\frac{T}{T^*}) + \delta\langle k\rangle(TI - T^*I^*\frac{T}{T^*})] \\
&= (1-\frac{T^*}{T})[\delta\langle k\rangle T^*S^*(\frac{TS}{T^*S^*} - \frac{T}{T^*}) + \delta\langle k\rangle T^*E^*(\frac{TE}{T^*E^*} - \frac{T}{T^*}) + \delta\langle k\rangle T^*I^*(\frac{TI}{T^*I^*} - \frac{T}{T^*})] \\
&= \delta\langle k\rangle T^*S^*(\frac{TS}{T^*S^*} - \frac{T}{T^*} - \frac{S}{S^*} + 1) + \delta\langle k\rangle T^*E^*(\frac{TE}{T^*E^*} - \frac{T}{T^*} - \frac{E}{E^*} + 1) \\
&\quad + \delta\langle k\rangle T^*I^*(\frac{TI}{T^*I^*} - \frac{T}{T^*} - \frac{I}{I^*} + 1).
\end{aligned}
$$

By further calculation, we obtain that

$$
\begin{aligned}
&\frac{\mathrm{d}V_1(t)}{\mathrm{d}t} + \frac{\mathrm{d}V_2(t)}{\mathrm{d}t} + \frac{\mathrm{d}V_3(t)}{\mathrm{d}t} + \frac{\mathrm{d}V_4(t)}{\mathrm{d}t} \\
\le\ & (1-\theta)\phi\langle k\rangle S^*I^*\left(2 - \frac{S^*}{S} + \frac{I}{I^*} - \frac{E}{E^*} - \frac{SIE^*}{S^*I^*E}\right) + \rho E^*\left(\frac{E}{E^*} - \frac{I}{I^*} - \frac{I^*E}{IE^*} - 1\right) \\
\le\ & (1-\theta)\phi\langle k\rangle S^*I^*\left(\ln\frac{S^*}{S} - \frac{S^*}{S} + \frac{I}{I^*} - \ln\frac{I}{I^*} + \ln\frac{E}{E^*} - \frac{E}{E^*} + 1\right) \\
& + \rho E^*\left(\frac{E}{E^*} - \ln\frac{E}{E^*} + \ln\frac{I}{I^*} - \frac{I}{I^*}\right).
\end{aligned}
$$

Then, it derives that

$$
\begin{aligned}
\frac{\mathrm{d}V(t)}{\mathrm{d}t} &= \frac{1}{(1-\theta)\phi\langle k\rangle S^*I^* + \rho E^*}\left(\frac{\mathrm{d}V_1(t)}{\mathrm{d}t} + \frac{\mathrm{d}V_2(t)}{\mathrm{d}t} + \frac{\mathrm{d}V_3(t)}{\mathrm{d}t} + \frac{\mathrm{d}V_4(t)}{\mathrm{d}t}\right) \\
&\le \frac{(1-\theta)\phi\langle k\rangle S^*I^*}{(1-\theta)\phi\langle k\rangle S^*I^* + \rho E^*}\left(\ln\frac{S^*}{S} - \frac{S^*}{S} + 1\right) \le 0.
\end{aligned}
$$

Moreover, $\frac{\mathrm{d}V}{\mathrm{d}t} = 0$ if and only if $S = S^*$, $E = E^*$, $I = I^*$, and $T = T^*$. In accordance with LaSalle's invariance principle [32], the endemic equilibrium E_3 of model (2.3) is globally asymptotically stable when $R_0 > 1$. □

Remark 3. *In [29], the authors proposed a susceptible-exposed-infected-media-recovered (SEIMR) rumor spreading model and analyzed the stability of its equilibrium. However, to the best of our knowledge, there has been relatively little research on the impact of true information spreader on rumor spreading. In contrast, this paper innovatively incorporates true information spreader into the rumor spreading model, constructing a new SEITR rumor spreading model. In our study, we mainly rely on the Routh-Hurwitz stability theorem, Lyapunov stability theory, and LaSalle's invariance principle to thoroughly investigate the stability of the equilibrium in this model.*

4. Optimal control

To eliminate the negative social impacts caused by rumors and curb their spreading trend, phased interventions should be implemented within a specific time horizon to reduce the scale of rumor spreaders and raise the proportions of immune individuals and genuine information disseminators, so as to drive the system toward a steady state. In this paper, the static transition parameters θ, ρ, and δ in the SEITR model are extended to time-varying control variables $\theta(t)$, $\rho(t)$, and $\delta(t)$. Compared with fixed constants, time-varying controls can be dynamically adjusted along with the evolution of public opinion, enabling precise regulation of the critical pathways for population state transitions.

The three types of time-varying controls correspond to differentiated intervention strategies for online public opinion: $\theta(t)$ denotes the intensity of media literacy popularization, which is adopted to reduce the probability that susceptible individuals believe and repost rumors; $\rho(t)$ represents the intensity of targeted clarification interventions to block the transformation from hesitant latent population to rumor spreaders; $\delta(t)$ stands for the incentive intensity for genuine information dissemination, guiding the public to actively spread authoritative rumor-refuting content. The synergy of the three variables forms a multi-level rumor intervention framework.

Assuming the finite control horizon is t_f, the optimal control objective function is defined as

$$J(\theta,\rho,\delta) = \int_0^{t_f} e^{-\sigma t}[E(t) + I(t) + T(t) + \frac{d_1}{2}\theta(t)^2 + \frac{d_2}{2}\rho(t)^2 + \frac{d_3}{2}\delta(t)^2]\,\mathrm{d}t. \tag{4.1}$$

The optimal control problem is shown below:

$$\begin{cases} \dfrac{\mathrm{d}S(t)}{\mathrm{d}t} = \Lambda - \phi\langle k\rangle S(t)I(t) - \delta(t)\langle k\rangle S(t)T(t) - \mu S(t), \\ \dfrac{\mathrm{d}E(t)}{\mathrm{d}t} = (1-\theta(t))\phi\langle k\rangle S(t)I(t) - \delta(t)\langle k\rangle E(t)T(t) - \rho(t)E(t) - \epsilon E(t) - \mu E(t), \\ \dfrac{\mathrm{d}I(t)}{\mathrm{d}t} = \theta(t)\phi\langle k\rangle S(t)I(t) + \rho(t)E(t) - \delta(t)\langle k\rangle I(t)T(t) - \epsilon I(t) - \mu I(t), \\ \dfrac{\mathrm{d}T(t)}{\mathrm{d}t} = \delta(t)\langle k\rangle T(t)(S(t)+E(t)+I(t)) - \mu T(t), \\ \dfrac{\mathrm{d}R(t)}{\mathrm{d}t} = \epsilon E(t) + \epsilon I(t) - \mu R(t). \end{cases} \tag{4.2}$$

The initial data for system (4.2) satisfies

$$S(0) = S_0 \geq 0, E(0) = E_0 \geq 0, I(0) = I_0 \geq 0, T(0) = T_0 \geq 0, R(0) = R_0 \geq 0, \tag{4.3}$$

where σ is the discount factor that reflects the weight attenuation of time on control costs and effects. d_1, d_2, d_3 are the weight coefficients of control costs, and $\theta(t), \rho(t), \delta(t)$ are measurable functions, where $\theta(t), \rho(t), \delta(t) \in U$ and $0 \leq \theta(t), \rho(t), \delta(t) \leq 1$, $\forall t \in [0, t_f]$.

4.1. Existence of optimal control

An optimal control exists as follows:

$$u^* = (\theta^*, \rho^*, \delta^*) \in U,$$

such that

$$J(\theta^*, \rho^*, \delta^*) = \min J(\theta(t), \rho(t), \delta(t)).$$

This optimal control solution is guaranteed under the following conditions:

(1) The control variables and state variables are all nonnegative.

(2) The control admissible set U is convex and closed.

(3) The integrand of the objective functional is convex within the admissible set U.

(4) The right of the state system is determined by a linear and bounded function of both the control variables and the state variables.

(5) The existence of normal numbers g_1, g_2 and $f > 1$ ensures that the integrand of the objective function satisfies the following inequality:

$$L(t;\theta;\rho;\delta) \geq g_1(|\theta|^2 + |\rho|^2 + |\delta|^2)^{\frac{f}{2}} - g_2.$$

The conditions (1)–(3) are obviously valid. Next, we prove the conditions (4) and (5).

Given that $N(t) = S(t) + E(t) + I(t) + T(t) + R(t)$, since the state variables sum to $N(t)$, it follows that each state variable is bounded above by $N(t)$.

$$S' < \Lambda, E' < (1-\theta(t))\phi\langle k\rangle SI, I' < \theta(t)\phi\langle k\rangle SI + \rho(t)E, T' < \delta(t)\langle k\rangle T(S+E+I), R' < \epsilon E + \epsilon I.$$

Therefore, condition (4) is proven.

For the final condition

$$L(t;\theta;\rho;\delta) \geq g_1(|\theta|^2 + |\rho|^2 + |\delta|^2)^{\frac{f}{2}} - g_2,$$

to satisfy this condition, we select $g_1 = \frac{e^{-\sigma t_0}}{2}\min\{d_1, d_2, d_3\}$ and any $g_2 \in R^+, f = 2$. This choice ensures that the condition holds.

4.2. Optimal control strategy

Theorem 4.1. *For the optimal control solution $(\theta^*, \rho^*, \delta^*)$ in model (2.3), there are corresponding adjoint variables $\lambda_i (i = 1, 2, \ldots, 5)$ that meet the following criteria:*

$$\begin{cases} \dfrac{d\lambda_1(t)}{dt} = \lambda_1[\phi\langle k\rangle I + \delta(t)\langle k\rangle T + \mu] - \lambda_2(1-\theta(t))\phi\langle k\rangle I - \lambda_3\theta(t)\phi\langle k\rangle I - \lambda_4\delta(t)\langle k\rangle T, \\ \dfrac{d\lambda_2(t)}{dt} = -e^{-\sigma t} + \lambda_2[\delta(t)\langle k\rangle T + \rho(t) + \epsilon + \mu] - \lambda_3\rho(t) - \lambda_4\delta(t)\langle k\rangle T - \lambda_5\epsilon, \\ \dfrac{d\lambda_3(t)}{dt} = -e^{-\sigma t} + \lambda_1\phi\langle k\rangle S - \lambda_2(1-\theta(t))\phi\langle k\rangle S + \lambda_3[-\theta(t)\phi\langle k\rangle S + \delta(t)\langle k\rangle T + \epsilon + \mu] - \lambda_4\delta(t)\langle k\rangle T - \lambda_5\epsilon, \\ \dfrac{d\lambda_4(t)}{dt} = -e^{-\sigma t} + \lambda_1\delta(t)\langle k\rangle S + \lambda_2\delta(t)\langle k\rangle E + \lambda_3\delta(t)\langle k\rangle I - \lambda_4[\delta(t)\langle k\rangle(S+E+I) - \mu], \\ \dfrac{d\lambda_5(t)}{dt} = \lambda_5\mu. \end{cases} \tag{4.4}$$

Furthermore, the optimal control strategy for model (2.3) *is represented by the triplet* $(\theta(t)^*, \rho(t)^*, \delta(t)^*)$*, which is defined as follows:*

$$\begin{cases} \theta^* = \min\{1, \max\{0, \dfrac{e^{\sigma t}}{d_1}[(\lambda_2 - \lambda_3)\phi\langle k\rangle SI + \omega_{11} - \omega_{12}]\}\}, \\ \rho^* = \min\{1, \max\{0, \dfrac{e^{\sigma t}}{d_2}[(\lambda_2 - \lambda_3)E + \omega_{21} - \omega_{22}]\}\}, \\ \delta^* = \min\{1, \max\{0, \dfrac{e^{\sigma t}}{d_3}[\langle k\rangle T(\lambda_1 S + \lambda_2 E + \lambda_3 I) - \lambda_4\langle k\rangle T(S+E+I) + \omega_{31} - \omega_{32}]\}\}. \end{cases} \tag{4.5}$$

Proof. The extended Hamiltonian function that incorporates a penalty term is defined as follows:

$$\begin{aligned}
H &= e^{-\sigma t}[E(t) + I(t) + T(t) + \frac{d_1}{2}\theta(t)^2 + \frac{d_2}{2}\rho(t)^2 + \frac{d_3}{2}\delta(t)^2] \\
&\quad +\lambda_1[\Lambda - \phi\langle k\rangle SI - \delta(t)\langle k\rangle ST - \mu S] \\
&\quad +\lambda_2[(1-\theta(t))\phi\langle k\rangle SI - \delta(t)\langle k\rangle ET - \rho(t)E - \epsilon E - \mu E] \\
&\quad +\lambda_3[\theta(t)\phi\langle k\rangle SI + \rho(t)E - \delta(t)\langle k\rangle IT - \epsilon I - \mu I] \\
&\quad +\lambda_4[\delta(t)\langle k\rangle T(S + E + I) - \mu T] + \lambda_5[\epsilon E + \epsilon I - \mu R] \\
&\quad -\omega_{11}\theta(t) - \omega_{12}(1-\theta(t)) - \omega_{21}\rho(t) - \omega_{22}(1-\rho(t)) - \omega_{31}\delta(t) - \omega_{32}(1-\delta(t)),
\end{aligned}$$

where $\omega_{ij} \geq 0$ is a penalty function. It limits $0 \leq \theta(t), \rho(t), \delta(t) \leq 1$ through complementary slackness and imposes heavy penalties near boundaries to discard unfeasible controls, making optimal strategies practical for public opinion management. Its complementary slackness conditions are

$$\omega_{11}(t)\theta^* = \omega_{12}(t)(1-\theta^*) = 0, \omega_{21}(t)\rho^* = \omega_{22}(t)(1-\rho^*) = 0, \omega_{31}(t)\delta^* = \omega_{32}(t)(1-\delta^*) = 0.$$

The synergetic system is

$$\frac{\mathrm{d}\lambda_1(t)}{\mathrm{d}t} = -\frac{\partial H}{\partial S(t)}, \frac{\mathrm{d}\lambda_2(t)}{\mathrm{d}t} = -\frac{\partial H}{\partial E(t)}, \frac{\mathrm{d}\lambda_3(t)}{\mathrm{d}t} = -\frac{\partial H}{\partial I(t)}, \frac{\mathrm{d}\lambda_4(t)}{\mathrm{d}t} = -\frac{\partial H}{\partial T(t)},$$

$$\frac{\mathrm{d}\lambda_5(t)}{\mathrm{d}t} = -\frac{\partial H}{\partial R(t)}, \lambda_i(T) = 0, i = 1, 2, \ldots, 5.$$

Taking the derivative of the Hamiltonian operator H with respect to the state variable $U = (\theta, \rho, \delta)$ and equating it to zero, we can observe that

$$\begin{cases}
\frac{\partial H}{\partial \theta} = e^{-\sigma t}d_1\theta(t) + (\lambda_3 - \lambda_2)\phi\langle k\rangle SI - \omega_{11} + \omega_{12} = 0, \\
\frac{\partial H}{\partial \rho} = e^{-\sigma t}d_2\rho(t) - \lambda_2 E + \lambda_3 E - \omega_{21} + \omega_{22} = 0, \\
\frac{\partial H}{\partial \delta} = e^{-\sigma t}d_3\delta(t) - \lambda_1\langle k\rangle ST - \lambda_2\langle k\rangle ET - \lambda_3\langle k\rangle IT + \lambda_4\langle k\rangle T(S + E + I) - \omega_{31} + \omega_{32} = 0.
\end{cases} \tag{4.6}$$

Derive the optimal control expression

$$\begin{cases}
\theta^* = \frac{e^{\sigma t}}{d_1}[(\lambda_2 - \lambda_3)\phi\langle k\rangle SI + \omega_{11} - \omega_{12}], \\
\rho^* = \frac{e^{\sigma t}}{d_2}[(\lambda_2 - \lambda_3)E + \omega_{21} - \omega_{22}], \\
\delta^* = \frac{e^{\sigma t}}{d_3}[\langle k\rangle T(\lambda_1 S + \lambda_2 E + \lambda_3 I) - \lambda_4\langle k\rangle T(S + E + I) + \omega_{31} - \omega_{32}].
\end{cases} \tag{4.7}$$

First, let's consider θ^*.
(1) On the set $0 < \theta^* < 1$, let $\omega_{11} = \omega_{12} = 0$, thus $\theta^* = \frac{e^{\sigma t}}{d_1}[(\lambda_2 - \lambda_3)\phi\langle k\rangle SI]$.
(2) On the set $\theta^* = 1$, let $\omega_{11} = 0$, thus $\theta^* = \frac{e^{\sigma t}}{d_1}[(\lambda_2 - \lambda_3)\phi\langle k\rangle SI - \omega_{12}]$.

(3) On the set $\theta^* = 0$, let $\omega_{12} = 0$, thus $\theta^* = \frac{e^{\sigma t}}{d_1}[(\lambda_2 - \lambda_3)\phi \langle k \rangle SI + \omega_{11}]$.
Therefore,

$$\theta^* = \min\{1, \max\{0, \frac{e^{\sigma t}}{d_1}[(\lambda_2 - \lambda_3)\phi \langle k \rangle SI + \omega_{11} - \omega_{12}]\}\}.$$

The optimal control ρ^* expresion is

$$\rho^* = \min\{1, \max\{0, \frac{e^{\sigma t}}{d_2}[(\lambda_2 - \lambda_3)E + \omega_{21} - \omega_{22}]\}\}.$$

The optimal control δ^* expression is

$$\delta^* = \min\{1, \max\{0, \frac{e^{\sigma t}}{d_3}[\langle k \rangle T(\lambda_1 S + \lambda_2 E + \lambda_3 I) - \lambda_4 \langle k \rangle T(S + E + I) + \omega_{31} - \omega_{32}]\}\}.$$

□

Remark 4. *The optimal control strategy proposed in this paper introduces a discount factor and a quadratic cost function into the objective function, which can distinguish the intervention value at different stages of rumor diffusion, strengthen the early prevention and control intensity, and ensure the uniqueness and stability of the optimal control solution. Combined with three-dimensional time-varying control variables, it can realize dynamic regulation and control of the evolution of public opinion. Compared with traditional control methods, this strategy can better balance the intervention timeliness and prevention and control costs, and solve the unreasonable problem of equal weight allocation at various stages.*

5. Numerical simulation and discussion

In this section, different parameters are chosen to verify the correctness of the theoretical analysis and the effectiveness of the control strategy. In addition, the established model is simulated using real-world data. Several groups of experimental parameters are presented below, with detailed values listed in Tables 2–4.

Table 2. System parameters.

parameters	$\langle k \rangle$	Λ	μ	θ	ϕ	δ	ρ	ϵ
Data 1 (E_0)	0.8	0.15	0.15	0.4	0.2	0.05	0.01	0.05
Data 2 (E_1)	0.8	0.15	0.15	0.6	0.4	0.4	0.2	0.2
Data 3 (E_2)	0.8	0.1	0.1	0.3	0.6	0.1	0.4	0.06
Data 4 (E_3)	0.8	0.15	0.15	0.7	0.9	0.3	0.01	0.05
Data 5	0.8	0.01	0.06	0.5	0.3	0.3	0.3	0.01

Table 3. Different initial conditions of $S(0), E(0), I(0)$, and $T(0)$.

parameters	$S(0)$	$E(0)$	$I(0)$	$T(0)$
Data 1 $N_{01\sim05}$ (E_0)	[0.75 ~ 0.55]	0.1	[0.05 ~ 0.25]	0.1
Data 2 $N_{11\sim15}$ (E_1)	[0.75 ~ 0.55]	0.1	0.1	[0.05 ~ 0.25]
Data 3 $N_{21\sim25}$ (E_2)	[0.85 ~ 0.65]	0.02	[0.08 ~ 0.28]	0.05
Data 4 $N_{31\sim35}$ (E_3)	[0.82 ~ 0.62]	0.11	[0.01 ~ 0.21]	0.06

Remark 5. *Each row in Table 3 corresponds to 5 sets of initial values ($N_{01\sim05}$, $N_{11\sim15}$, $N_{21\sim25}$, $N_{31\sim35}$): interval values are sampled across the range with a step size of 0.05, while a single value means the five sets of initial values are identical; fixed values for each group are set based on the dynamic characteristics of corresponding equilibrium points and verification objectives, and the design of fixing non-critical variables and testing core variables within intervals avoids multi-variable interference and matches the characteristics of each equilibrium point accurately.*

5.1. Stability of the equilibrium solutions

In this section, we verify the stability conditions of equilibrium points given in the previous theoretical part, and plot the local asymptotic stability curves of each equilibrium point as well as the three-dimensional phase portraits of the model under different initial conditions.

Using Data 1 in Table 2 with initial densities $S(0) = 0.65$, $E(0) = 0.2$, $I(0) = 0.1$, and $T(0) = 0.05$, we calculate the basic reproduction number as $R_0 \approx 0.34 < 1$. According to Theorem 3.1, the stability condition of the rumor-free equilibrium E_0 is satisfied, implying that E_0 is locally asymptotically stable. Figure 2(a) presents the time-series plots of the densities $S(t)$, $E(t)$, $I(t)$, and $T(t)$ over time, showing that model (2.3) eventually converges to the steady state.

For Data 2 in Table 2 with initial densities $S(0) = 0.7$, $E(0) = 0.1$, $I(0) = 0.1$, and $T(0) = 0.1$, we obtain $R_{01} \approx 0.68 < 1$, $R_{02} \approx 2.13 > 1$ and $\phi = 0.4 < \frac{\delta(\delta\langle k\rangle\Lambda+\epsilon\mu)(\delta\langle k\rangle\Lambda+\rho\mu+\epsilon\mu)}{\mu^2(\theta\delta\langle k\rangle\Lambda+\theta\epsilon\mu+\rho\mu)} = 1.95$. Based on Theorem 3.3, the stability condition of the boundary equilibrium E_1 is fulfilled, so E_1 is locally asymptotically stable, and the model also converges to the steady state (see Figure 2(b)).

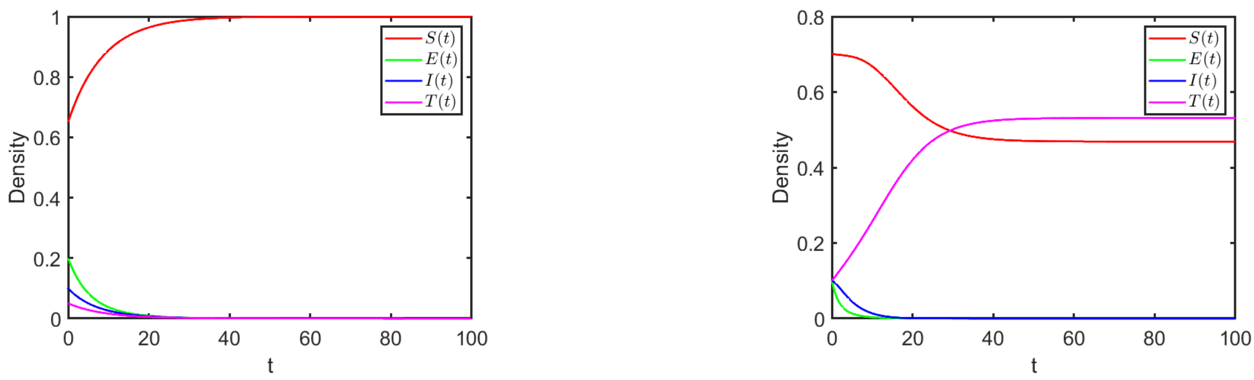

(a) (b)

Figure 2. Local stability of the rumor-free equilibrium E_0 and the boundary equilibrium E_1.

Using Data 3 in Table 2 with initial densities $S(0) = 0.67$, $E(0) = 0.2$, $I(0) = 0.03$, and $T(0) = 0.1$, we obtain $R_{01} = 2.4 > 1$ and $R_{02} = 0.8 < \min\{1, \frac{\phi\langle k\rangle\Lambda R_{01}(\rho+\epsilon+\mu)}{(\rho+\epsilon+\mu)[\phi\langle k\rangle\Lambda+\mu^2 R_{01}(R_{01}-1)]+\phi\mu\langle k\rangle\Lambda(1-\theta)(R_{01}-1)}\} = 1$. According to Theorem 3.5, the stability condition for the equilibrium E_2 is satisfied, so E_2 is locally asymptotically stable. As shown in Figure 3(a), model (2.3) eventually converges to the steady state.

Using Data 4 in Table 2 with initial densities $S(0) = 0.9$, $E(0) = 0.02$, $I(0) = 0.01$, and $T(0) = 0.7$, we obtain $R_0 \approx 2.57 > 1$ and $\frac{\theta\phi\mu}{\delta\epsilon} = 6.3 > 1$, which satisfies the existence condition of the equilibrium E_3. As shown in Figure 3(b), the existence of the positive equilibrium solution of model (2.3) is verified.

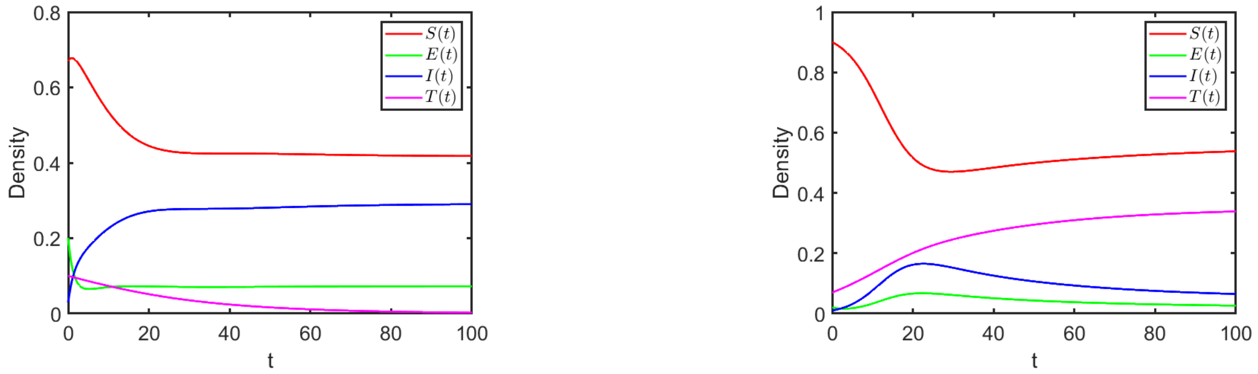

(a) (b)

Figure 3. Local stability of the boundary equilibrium E_2 and the endemic equilibrium E_3.

Based on the initial value data in Table 3, the three-dimensional phase portraits of the four equilibrium points are plotted respectively (Figures 4 and 5). For each group of data, five different initial densities are set to demonstrate the evolutionary trajectories of $S(t)$, $I(t)$, and $T(t)$ under different initial conditions. The results show that the trajectories of the model eventually converge to the corresponding equilibrium point regardless of the variation in initial values.

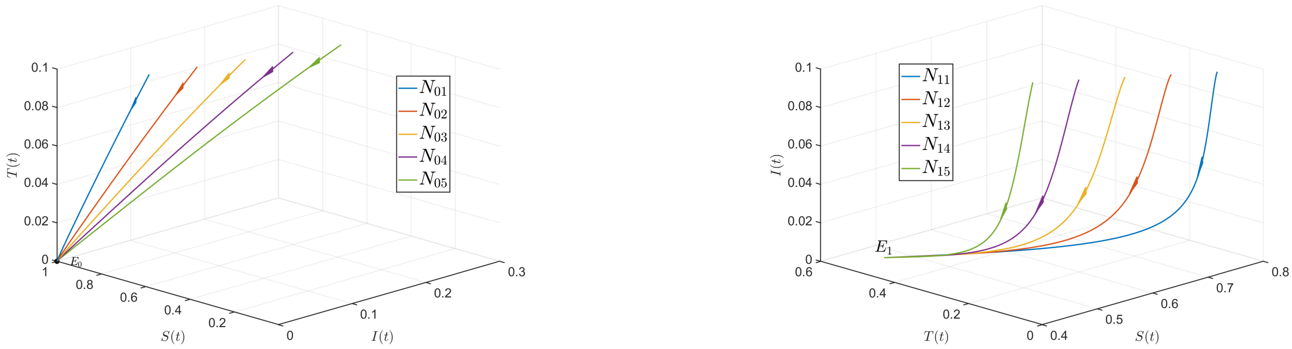

(a) (b)

Figure 4. Three-dimensional phase portraits of the rumor-free equilibrium E_0 and the boundary equilibrium E_1.

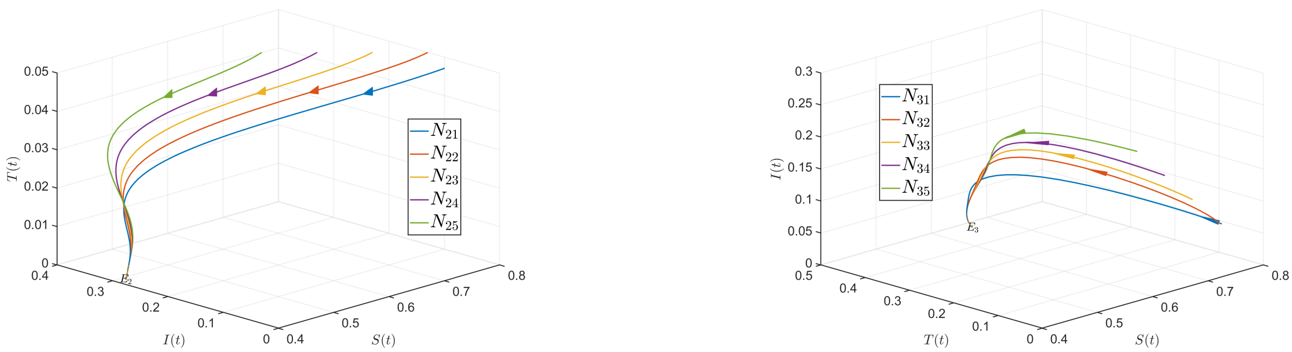

(a) (b)

Figure 5. Three-dimensional phase portraits of the boundary equilibrium E_2 and the endemic equilibrium E_3.

5.2. *Impact of key parameters on the model* (2.3)

Based on the parameter settings listed in Table 4, this section separately investigates the effects of the rumor transmission rate θ, contact rate ϕ, conversion rate of truth spreaders δ, average network degree $\langle k \rangle$, and initial value of truth spreaders $T(0)$ on the evolutionary law of rumor propagation.

Table 4. Impact of key parameters.

Figure	Λ	μ	$\langle k \rangle$	ϕ	θ	δ	ρ	ϵ
Figure 6(a) (θ)	0.01	0.01	0.8	0.9	—	0.01	0.01	0.01
Figure 6(b) (ϕ)	0.015	0.015	0.8	—	0.8	0.02	0.01	0.01
Figure 7(a) (δ)	0.01	0.01	0.8	0.7	0.8	—	0.01	0.01
Figure 7(b) ($\langle k \rangle$)	0.015	0.015	—	0.75	0.85	0.12	0.01	0.04
Figure 8 (T_0)	0.01	0.01	0.8	0.5	0.85	0.1	0.01	0.02

Figure 6 demonstrates the effects of rumor spread rate θ and contact rate ϕ on the number of rumor spreaders $I(t)$. The results show that as θ and ϕ increase, both the density and peak of $I(t)$ increase, and the time to reach the peak decreases.

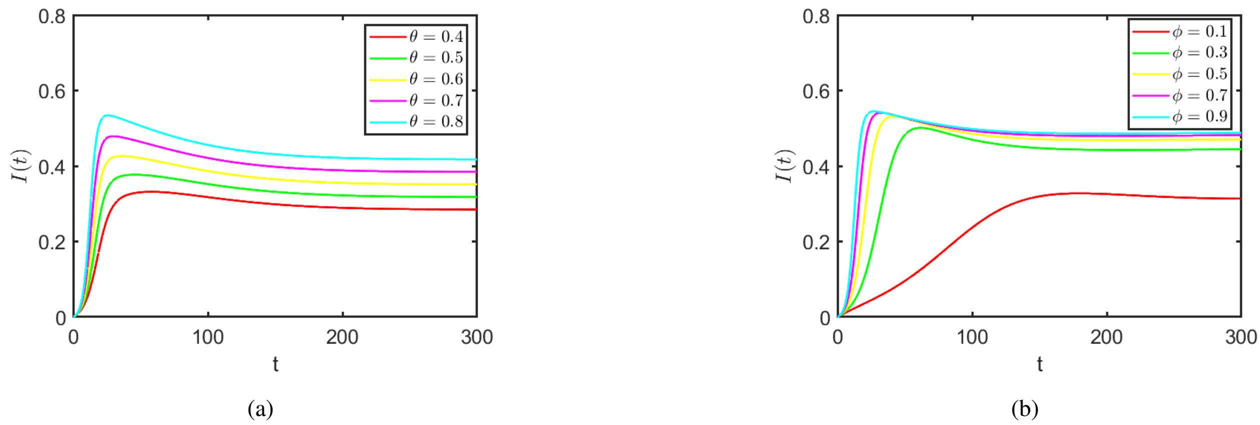

Figure 6. The evolution of the densities of $I(t)$ under varying θ and ϕ.

Figure 7(a) shows the impact of different values of the true information spreader conversion rate δ on the rumor spreader $I(t)$. The results indicate that as δ increases, both the density and peak of $I(t)$ decrease, and the duration of rumor spreading is shortened. Therefore, increasing the delta parameter can effectively reduce the number of rumor spreaders.

Figure 7(b) shows how rumor spread density changes with different $\langle k \rangle$ values. The study founds that as $\langle k \rangle$ increases, the density of $I(t)$ reaches its peak more quickly. The average degree of the network indicates the closeness of connections between users. Therefore, in a social network, the closer the connections among users, the faster the rumor will spread, and the wider its spread will be.

Figure 8 shows the impact of different initial values $T(0)$ on the number of rumor spreaders $I(t)$. The results indicate that as the initial value $T(0)$ increases, the peak of $I(t)$ decreases. This is because a larger initial value for true information spreaders means more people will spread the true information, which in turn slows down the speed of rumor spreading. Therefore, increasing the initial value of true information spreaders can effectively control the spread of rumors.

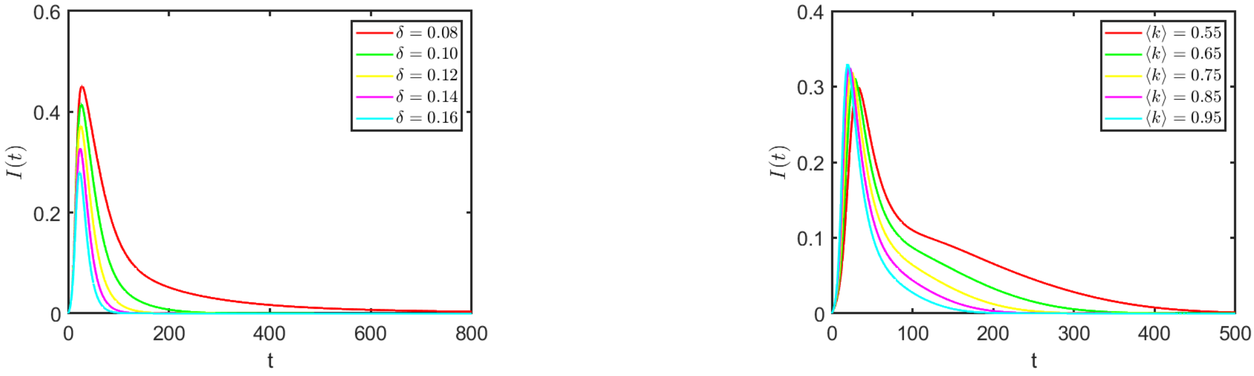

(a) (b)

Figure 7. The evolution of the densities of $I(t)$ under varying δ and $\langle k \rangle$.

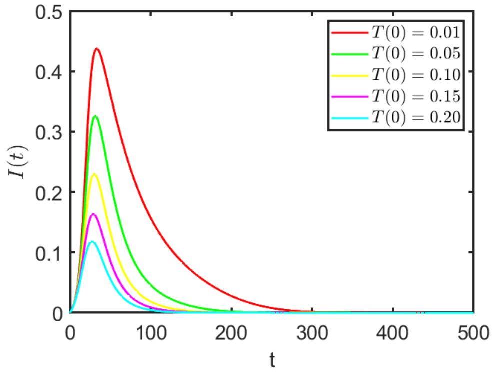

Figure 8. The evolution of the densities of $I(t)$ under varying $T(0)$.

5.3. *Effectiveness of optimal control*

Based on the optimal control model (4.2), Data 5 in Table 2 is selected with initial densities $S(0)$=0.5, $E(0) = 0.2$, $I(0) = 0.2$, $T(0) = 0.05$, and $R(0) = 0.05$. In the objective function, we set $\sigma = 0.01$, $d_1 = 0.1$, $d_2 = 0.1$, and $d_3 = 0.5$. Figure 9 compares the evolutionary curves of five types of populations under uncontrolled condition, single θ control, single ρ control, single δ control, and three-dimensional joint control.

Simulation results reveal obvious deficiencies of the three single control strategies: Single θ and single ρ can only slightly reduce the peak value of rumor spreaders; although single δ can expand the scale of truth spreaders, it fails to control susceptible and exposed populations at the source, resulting in relatively high peak scale and long duration of rumors. The three-dimensional joint control realizes multi-layer synchronous intervention, where θ reduces the transformation from susceptible individuals to rumor spreaders, ρ cuts off the propagation chain of exposed population, and δ accelerates the conversion of all types of populations into truth spreaders. It can be observed from the curves that under joint control, $E(t)$ decays at the fastest rate, the peak value and duration of $I(t)$ are greatly reduced, the scale of $T(t)$ is remarkably larger than that under all single control schemes, and $R(t)$

declines more rapidly, which thoroughly blocks the rumor transmission chain. In conclusion, single intervention delivers limited governance performance, while the collaborative control of θ, ρ, and δ balances governance effectiveness and intervention cost, providing quantitative theoretical support for multi-dimensional joint governance of online rumors.

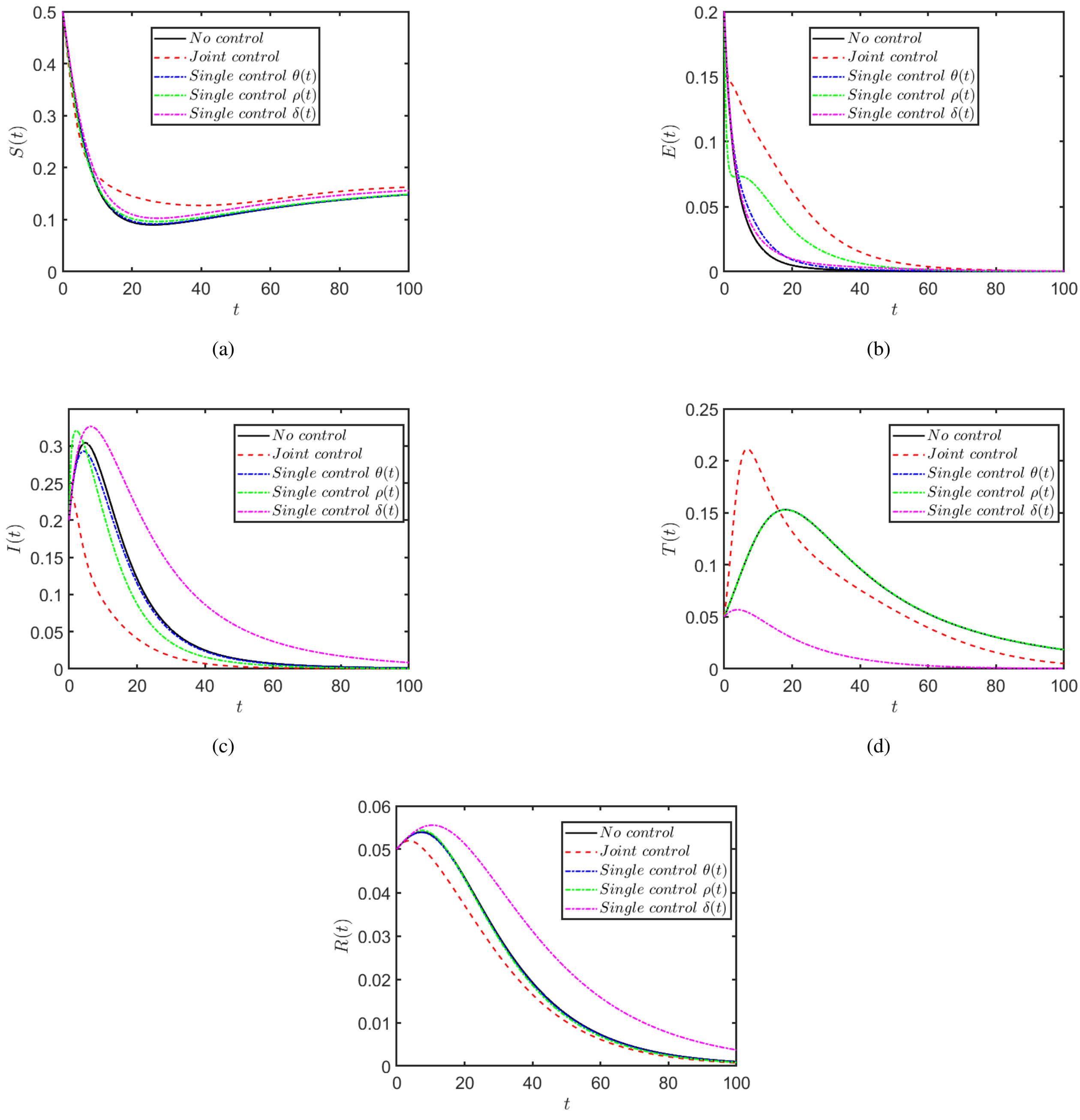

(a) (b) (c) (d) (e)

Figure 9. The impact of optimal control on rumor propagation.

Figure 10 presents the time evolution of the optimal control variables and the control cost. As shown in Figure 10(a), the optimal control variables exhibit dynamic adjustment characteristics: The core control variable $\delta(t)$ remains at a high level in the initial stage to rapidly increase truth spreaders and suppress rumors, stabilizes within a balanced interval of 0.2–0.3 in the medium term, and gradually decreases to 0 in the later stage as the rumor is controlled; $\rho(t)$ stays at a high level initially to block the transition of exposed individuals to rumor spreaders, and then drops rapidly to 0 after the exposed population decays quickly; $\theta(t)$ maintains an extremely low level throughout the process, since the suppression effect of truth spreaders is sufficient to block the transition from susceptible individuals to rumor spreaders without additional cost, which reflects the dynamic balance of the control strategy between effect priority and cost optimality. As can be seen from Figure 10(b), the control cost $J(t)$ accumulates gradually over time, with a faster growth rate in the early stage than in the later stage.

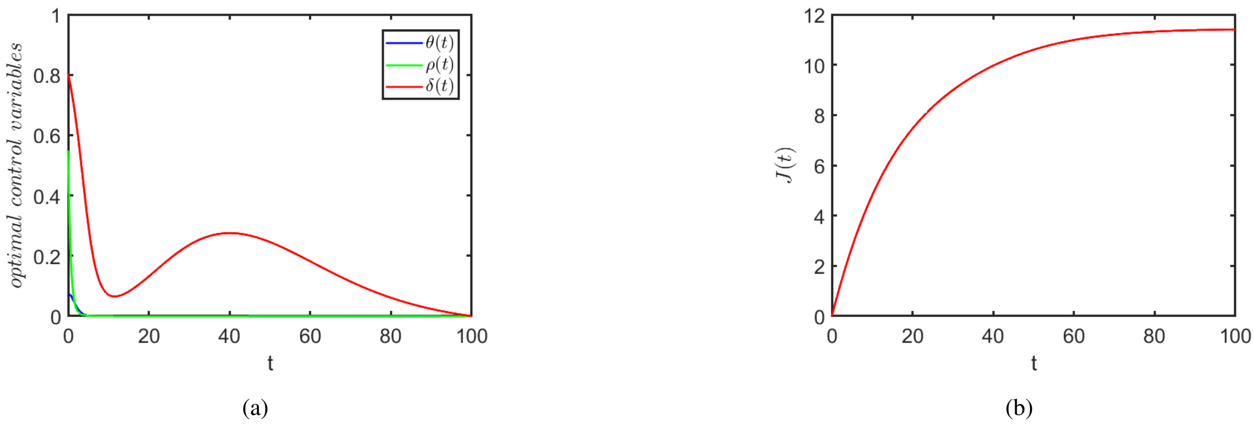

Figure 10. The time evolution of the optimal control variables and the control cost.

Remark 6. *In Figure 10(b), the cost functional $J(t)$ keeps rising. This curve represents the cumulative integral value from time 0 to time t instead of the instantaneous cost. The optimization objective of this paper is to minimize the terminal total cost $J(t_f)$. The control cost and rumor-induced losses over the whole time horizon are continuously incorporated into the integral, so $J(t)$ increases monotonically, and its growth rate slows down in the later stage and finally converges to a stable upper bound.*

5.4. Practical applications of the model

This subsection uses the real-world dataset provided in Ref. [33] to verify the effectiveness of the model proposed in this paper. The background of the selected rumor incident is described as follows: On December 22, 2017, a piece of news claiming that a tourist dragged an elephant's tail in Thailand, causing the accompanying tour guide to be trampled to death by the elephant went viral on Sina Weibo. Closely related to public life and attracting extensive social attention, this story quickly sparked heated discussions across the whole network. It was not until December 25 that the Thai police issued an official clarification statement, confirming that the viral news was inconsistent with the facts and the tourist had neither dragged nor harassed the elephant.

We counted the hourly volume of reposts, comments, and likes generated by this rumor after its outbreak. Combined with the statistical data, we regard the period from 8:00 to 22:00 as the effective time window for rumor propagation. The detailed raw statistics are presented in Table 5.

Table 5. The number of reposts, comments, and likes.

Time	Reposts	Comments	Likes	Time	Reposts	Comments	Likes
1h	85	163	111	23h	57	135	412
2h	89	69	60	24h	176	108	158
3h	1117	2027	2429	25h	226	580	1170
4h	902	2165	1506	26h	44	83	119
5h	220	839	719	27h	34	19	29
6h	1914	3304	4022	28h	79	161	149
7h	1050	3014	3444	29h	39	52	75
8h	919	418	390	30h	50	124	205
9h	299	539	490	31h	119	280	256
10h	92	285	189	32h	4	2	1
11h	20	24	71	33h	20	17	22
12h	346	1067	3978	34h	48	43	47
13h	40	126	206	35h	86	180	428
14h	562	831	2672	36h	3	1	1
15h	381	1400	5114	37h	13	8	22
16h	214	264	385	38h	30	27	97
17h	182	516	1152	39h	2	0	0
18h	83	179	259	40h	2	0	0
19h	13	8	14	41h	22	36	24
20h	31	37	48	42h	0	0	0
21h	6	7	12	43h	0	0	0
22h	294	390	386	44h	0	0	0

It can be intuitively observed from Figure 11(a) that there is a significant positive correlation among the number of reposts, comments, and likes. Among them, both the reposts and comments reach their peak values at the 6th hour, while the peak of likes appears at the 15th hour. Figure 11(b) further shows the cumulative total of reposts, comments, and likes per hour.

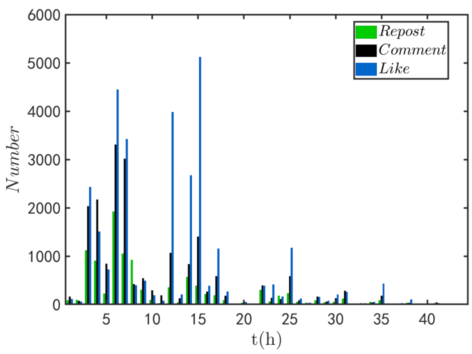

(a)

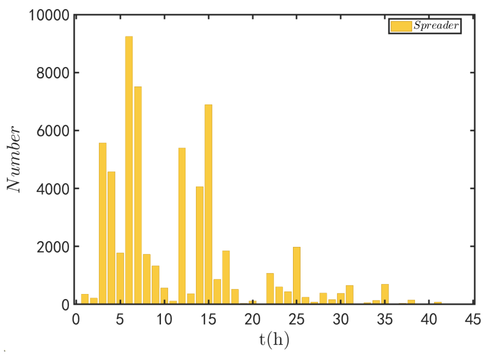

(b)

Figure 11. The number of reposts, comments, and likes.

To make the model more consistent with real data, we select the parameters $\langle k \rangle = 0.5$, $\Lambda = 0.08$, $\mu = 0.06$, $\theta = 0.7$, $\phi = 0.85$, $\delta = 0.2$, $\rho = 0.08$, and $\epsilon = 0.01$. Figure 12 simulates the evolution of this rumor propagation. It can be seen from the figure that the variation trajectory of the rumor-infected individuals' density is basically consistent with the overall trend of the real data, indicating that the model constructed in this paper can well reflect the actual propagation process of rumors.

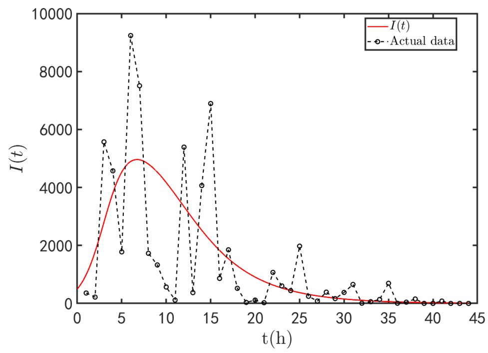

Figure 12. Simulation based on real rumor data.

To eliminate magnitude interference, all data are normalized to $[0, 1]$. The fitting indexes are MSE=0.0865, RMSE = 0.2941, MAE = 0.1700, and Pearson correlation $r = 0.6445$. The moderate positive correlation demonstrates that the SEITR model captures the overall rise-fall trend of real rumors, while moderate deviation arises from the homogeneous mixing assumption of the compartment model.

5.5. Sensitivity analysis

In the section, our main task is to explore how various parameters in the model affect the basic reproduction number, a process known as sensitivity analysis. First, we introduce the definition of sensitivity analysis as follows [34].

Definition 1. *The normalized forward sensitivity index of a variable u, which depends on differentiably parameter q, is defined as*

$$\gamma_q^u = \frac{\partial u}{\partial q} \times \frac{q}{u}.$$

Since the value of R_0 is the maximum of R_{01} and R_{02}, it is necessary to conduct sensitivity analysis on R_{01} and R_{02} separately. Here, we only present the results of R_{01} due to their similarity. Through straightforward calculations, we have obtained the sensitivity indices of the model (2.3) parameters to R_{01}, as shown in Table 6, and the values of the parameters are set according to Data 1 in Table 2.

Table 6. Sensitivity index of R_{01} to parameters values.

Parameter	ϕ	$\langle k \rangle$	Λ	θ	ϵ	ρ	μ
Sensitivity index	1	1	1	0.889	-0.266	0.063	-1.797

Next, the influence extent of parameters related to R_{01} on the SEITR rumor spreading model (2.3) can be evaluated quantitatively by sensitivity analysis in Table 6. If we adjust the parameters by 1%, the results in Table 6 indicate the proportional change in the variable.

Figure 13 presents the impact of model parameters on the basic reproduction number R_{01}. It can be more intuitively observed that higher transmission rate θ and conversion rate ρ lead to a larger R_{01}, which exacerbates rumor propagation, whereas a higher recovery rate ϵ results in a smaller R_{01}, effectively mitigating the spread of rumors.

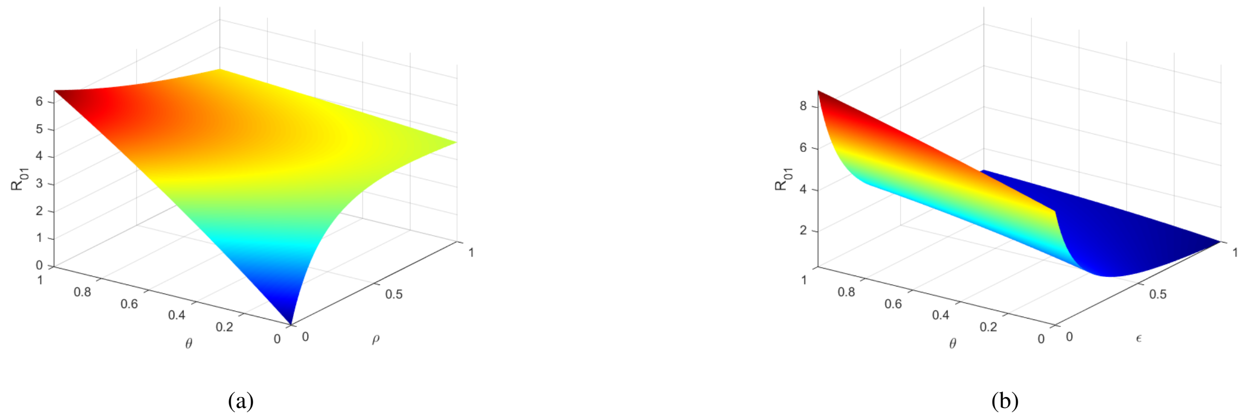

Figure 13. The relationship between the basic reproduction number R_{01} and θ, ρ, and ϵ.

Remark 7. *In summary, the most effective strategy to reduce R_{01} is to increase the emigration rate μ and the recovery rate ϵ. This can be achieved through educational campaigns, the implementation of government punitive measures, and the timely release of official information. Additionally, reducing the coming rate can be facilitated by online public opinion supervision and education. Meanwhile, lowering the spread rate can be accomplished by monitoring disseminators and, if necessary, imposing penalties.*

6. Conclusions

In this paper, an SEITR rumor propagation model is established by introducing both hesitant individuals and truth spreaders simultaneously. The basic reproduction number R_0 of the model is derived using the next-generation matrix method, and the stability of each equilibrium is analyzed by means of the Routh-Hurwitz criterion and Lyapunov stability theory. Furthermore, by dynamically adjusting control variables within a finite time interval, the optimal control strategy of the model is analyzed based on Pontryagin's minimum principle to suppress rumor propagation. Finally, numerical simulations are carried out to verify the correctness of the theoretical results, the effectiveness of the optimal control strategy, and the influence of different parameters in the model. The results show that dynamically adjusting model parameters, prioritizing the increase of truth spreaders, and blocking rumor transition pathways can effectively suppress rumor propagation. This study deepens the understanding of rumor propagation mechanisms and provides theoretical support for the formulation of control strategies.

The model in this paper adopts a homogeneous network assumption and fixed parameters. The three time-varying controls only correspond to single intervention channels including science popularization, rumor refutation, and genuine information promotion, without incorporating multi-party collaborative governance mechanisms such as official media releases, platform supervision, and netizen selfdiscipline. Simulations are only conducted based on a single public opinion case, lacking comparative verification across multiple types of rumors, and random disturbances and time-delay effects are not considered. Future research can introduce heterogeneous complex networks and stochastic time-delay propagation models, expand multi-agent joint controls to construct multi-objective optimal control schemes, collect real public opinion data of various rumor types for fitting and verification, and integrate machine learning to realize real-time dynamic regulation of public opinion.

Author contributions

Yuzhen Zhao: Conceptualization, Methodology, Formal analysis, Writing–original draft, Writing–review and editing; Jinling Wang: Supervision, Project administration, Writing–review and editing; Jiarong Li: Supervision.

Use of Generative-AI tools declaration

No generative artificial intelligence large language models were adopted for manuscript writing, model derivation, simulation and data analysis.

Acknowledgments

This work was supported in part by the National Natural Science Foundation of People's Republic of China under Grant 62366049, in part by Natural Science Foundation of Xinjiang Uygur Autonomous Region (No. 2025D01C32), and in part by the Natural Science Foundation of Fujian Province of China (2024J01725).

Conflict of interest

The authors declare there is no conflict of interest.

References

1. L. Huo, S. Chen, Rumor propagation model with consideration of scientific knowledge level and social reinforcement in heterogeneous network, *Physica A*, **559** (2020), 125063. https://doi.org/10.1016/j.physa.2020.125063
2. D. Zanette, M. Kuperman, Effects of immunization in small-world epidemics, *Physica A*, **309** (2002), 445–452. https://doi.org/10.1016/S0378-4371(02)00618-0
3. Y. Moreno, M. Nekovee, A. Pacheco, Dynamics of rumor spreading in complex networks, *Phys. Rev. E*, **69** (2004), 066130. https://doi.org/10.1103/PhysRevE.69.066130
4. D. Daley, D. Kendall, Stochastic rumours, *IMA J. Appl. Math.*, **1** (1965), 42–55. https://doi.org/10.1093/imamat/1.1.42
5. D. Maki, M. Thompson, *Mathematical models and applications: with emphasis on the social, life and management sciences*, New Jersey: Prentice Hall, 1973.

6. L. Zhu, B. Wang, Stability analysis of a SAIR rumor spreading model with control strategies in online social networks, *Inform. Sciences*, **526** (2020), 1–19. https://doi.org/10.1016/j.ins.2020.03.076
7. L. Huo, Y. Cheng, The impact of media coverage and emergency strategies on the rumor spreading, *Discrete Dyn. Nat. Soc.*, **2018** (2018), 4137129. https://doi.org/10.1155/2018/4137129
8. J. Wang, H. Jiang, T. Ma, C. Hu, Global dynamics of the multi-lingual SIR rumor spreading model with cross-transmitted mechanism, *Chaos Soliton. Fract.*, **126** (2019), 148–157. https://doi.org/10.1016/j.chaos.2019.05.027
9. M. Nekovee, Y. Moreno, G. Bianconi, M. Marsili, Theory of rumour spreading in complex social networks, *Physica A*, **374** (2007), 457–470. https://doi.org/10.1016/j.physa.2006.07.017
10. D. Zanette, Dynamics of rumor propagation on small-world networks, *Phys. Rev. E*, **65** (2002), 041908. https://doi.org/10.1103/PhysRevE.65.041908
11. D. Zanette, Critical behavior of propagation on small-world networks, *Phys. Rev. E*, **64** (2001), 050901. https://doi.org/10.1103/PhysRevE.64.050901
12. P. Jia, C. Wang, G. Zhang, J. Ma, A rumor spreading model based on two propagation channels in social networks, *Physica A*, **524** (2019), 342–353. https://doi.org/10.1016/j.physa.2019.04.163
13. C. Wang, G. Wang, X. Luo, H. Li, Modeling rumor propagation and mitigation across multiple social networks, *Physica A*, **535** (2019), 122240. https://doi.org/10.1016/j.physa.2019.122240
14. Y. Lan, Z. Lian, R. Zeng, D. Zhu, Y. Xia, M. Liu, et al., A statistical model of the impact of online rumors on the information quantity of online public opinion, *Physica A*, **541** (2020), 123623. https://doi.org/10.1016/j.physa.2019.123623
15. Q. Liu, T. Li, M. Sun, The analysis of an SEIR rumor propagation model on heterogeneous network, *Physica A*, **469** (2017), 372–380. https://doi.org/10.1016/j.physa.2016.11.067
16. S. Kang, X. Hou, Y. Hu, H. Liu, Dynamical analysis and optimal control of the developed information transmission model, *PLoS ONE*, **17** (2022), e0268326. https://doi.org/10.1371/journal.pone.0268326
17. G. Liu, J. Chen, Z. Liang, Z. Peng, J. Li, Dynamical analysis and optimal control for a SEIR model based on virus mutation in WSNs, *Mathematics*, **9** (2021), 929. https://doi.org/10.3390/math9090929
18. S. Chen, H. Jiang, L. Li, J. Li, Dynamical behaviors and optimal control of rumor propagation model with saturation incidence on heterogeneous networks, *Chaos Soliton. Fract.*, **140** (2020), 110206. https://doi.org/10.1016/j.chaos.2020.110206
19. K. Karumathil, S. Kundu, P. Konar, Dynamic analysis of rumor propagation: media effect, forgetting and remembering mechanisms, *Eur. Phys. J. Plus*, **141** (2026), 161. https://doi.org/10.1140/epjp/s13360-026-07381-6
20. P. Li, F. Hu, F. Li, Y. Zhao, Y. Song, SEIAR rumor spreading model with antagonistic states in hypernetworks, *Appl. Math. Comput.*, **508** (2026), 129637. https://doi.org/10.1016/j.amc.2025.129637
21. K. Du, R. Fan, D. Wang, X. Xie, X. Xu, J. Lin, Competitive information spreading model in two-layer networks considering dual debunking mechanisms and time lag effects, *Physica A*, **665** (2025), 130479. https://doi.org/10.1016/j.physa.2025.130479

22. W. Zheng, Y. Sun, X. Zhang, K. Wang, F. Liu, Research on rumor and anti rumor propagation models based on quantum superposition states, *Sci. Rep.*, **15** (2025), 13220. https://doi.org/10.1038/s41598-025-96006-6
23. M. Wang, Y. Hu, Dynamic analysis and control measures of rumor propagation model considering true individuals and public opinion individuals, *Inform. Sciences*, **676** (2024), 120779. https://doi.org/10.1016/j.ins.2024.120779
24. J. Zhang, H. Guo, W. Jing, Z. Jin, Dynamic analysis of rumor propagation model based on true information spreader (Chinese), *Acta Phys. Sin.*, **68** (2019), 150501. https://doi.org/10.7498/aps.68.20190191
25. L. Zhu, Y. Ding, S. Shen, Green behavior propagation analysis based on statistical theory and intelligent algorithm in data-driven environment, *Math. Biosci.*, **379** (2025), 109340. https://doi.org/10.1016/j.mbs.2024.109340
26. H. Sha, L. Zhu, Dynamic analysis of pattern and optimal control research of rumor propagation model on different networks, *Inform. Process. Manag.*, **62** (2025), 104016. https://doi.org/10.1016/j.ipm.2024.104016
27. H. Ali, S. Owyed, I. Ameen, Fractional optimal control problem and stability analysis of rumor spreading model with effective strategies, *Mathematics*, **13** (2025), 1746. https://doi.org/10.3390/math13111746
28. A. Jain, J. Dhar, V. Gupta, Optimal control of rumor spreading model on homogeneous social network with consideration of influence delay of thinkers, *Differ. Equ. Dyn. Syst.*, **31** (2023), 113–134. https://doi.org/10.1007/s12591-019-00484-w
29. H. Guo, X. Yan, Y. Niu, J. Zhang, Dynamic analysis of rumor propagation model with media report and time delay on social networks, *J. Appl. Math. Comput.*, **69** (2023), 2473–2502. https://doi.org/10.1007/s12190-022-01829-5
30. P. van den Driessche, J. Watmough, Reproduction numbers and sub-threshold endemic equilibria for compartmental models of disease transmission, *Math. Biosci.*, **180** (2002), 29–48. https://doi.org/10.1016/S0025-5564(02)00108-6
31. R. Clark Robinson, *An introduction to dynamical systems: continuous and discrete*, Providence: American Mathematical Society, 2012.
32. J. LaSalle, Stability theory for ordinary differential equations, *J. Differ. Equations*, **4** (1968), 57–65. https://doi.org/10.1016/0022-0396(68)90048-X
33. S. Yu, Z. Yu, H. Jiang, S. Yang, The dynamics and control of 2I2SR rumor spreading models in multilingual online social networks, *Inform. Sciences*, **581** (2021), 18–41. https://doi.org/10.1016/j.ins.2021.08.096
34. N. Chitnis, J. Hyman, J. Cushing, Determining important parameters in the spread of malaria through the sensitivity analysis of a mathematical model, *Bull. Math. Biol.*, **70** (2008), 1272–1296. https://doi.org/10.1007/s11538-008-9299-0